International Journal of Mathematical, Engineering and Management Sciences
Vol. 10, No. 5, 1365-1396, 2025
https://doi.org/10.33889/IJMEMS.2025.10.5.065

Ram Arti Publishers

A Techno-Economic Analysis of Solar/Wind/Hydrokinetic Turbine-Based Green Hydrogen and Electricity-Generated Standalone DC Microgrid for Remote Area Applications

Saikumar Puppala
Department of Electrical Engineering,
National Institute of Technology, Meghalaya, 793003, Meghalaya, India.
Corresponding author: pkumar@nitm.ac.in

Piyush Pratap Singh
Department of Electrical Engineering,
National Institute of Technology, Meghalaya, 793003, Meghalaya, India.
E-mail: piyushpratap.singh@nitm.ac.in

Devendra Potnuru
Department of Electrical Engineering,
North Eastern Regional Institute of Science and Technology, Nirjuli (Itanagar), 791109, Arunachal Pradesh, India.
E-mail: dpn@nerist.ac.in

(Received on November 13, 2024; Revised on February 21, 2025 & April 23, 2025, Accepted on May 8, 2025)

Abstract
Access to reliable and sustainable energy is crucial for developing remote communities. Many remote communities need help accessing traditional grid infrastructure, resulting in energy deficits and reliance on expensive and harmful fuel sources. This article investigates the feasibility, planning, optimal, technical, and economic analysis of solar, wind, and hydrokinetic energy with battery storage-based standalone DC microgrids to produce green hydrogen and electricity for remote area applications. The proposed DC microgrid with net-zero emission and using sustainable resources in a remote area (Dayarthi and Rachakilam villages) in Andhra Pradesh, India, considers the DC loads. Optimal, technical, economic, and feasibility analysis has been explored to highlight the significance of the proposed configuration with the hybrid optimization of multiple energy resources (HOMER) simulation and the environment by taking the geographic regions' climatic data. The feasibility analysis considers three scenarios and demonstrates the performance characteristics with attributes such as net present cost (NPC), levelized cost of electricity (LCOE), levelized cost of hydrogen (LCOH), and capacity shortage factor (CSF). The feasibility analysis illustrates an efficient and cost-effective system configuration compared to the other integrated DC microgrid scenarios for generating green hydrogen and electricity for remote area applications. Also, the research explores sustainable energy access and proposes resilient and eco-friendly energy solutions for remote areas.

Keywords- Green hydrogen generation, Renewable energy resources, DC microgrid, Techno-economic analysis, Remote area applications.

Nomenclatures

A_{HKT}	Rotating hydrokinetic turbine blade area, in m^2.
B_E & A_E	Curve consumption coefficients in kW/kg/h.
$C_{Ear.,Eq.,m}$	Total equipment monthly revenue at year m in ($).
CRF( )	A function returning the capital recovery factor.
$C_{NPC,\ Pro.}$	Total project NPC in ($).
$C_{NPC,\ Tot.\ Eq.}$	NPC of the total equipment ($).
$C_{Sp.,Eq.,m}$	Total equipment monthly spends at a year m in ($).
$C_{Tot.,Anu.}$	Total annualized cost in ($).
$C_{\rho HKT}$	Hydrokinetic turbine efficiency coefficient.

d_f	Fraction of discount.
E_{Served}	Total electric load aided in kWh/yr.
F	Faraday's constant.
F_{SPV}	The percentage determining factor is set at 80%.
G_T	The current time step indicates the solar radiation incident on the PV array in kW/m^2.
$G_{T,stc}$	The standard test condition for incident radiation is 1 kW/m^2.
H	The period of time over which the hydrokinetic turbine is expected to generate energy and be forecast.
I_{ele}	The current in an electrolyzer.
i	Actual discount rate.
J	Total number of Equipment.
m	Number of years.
$M_{Hydrogen}$	Total hydrogen produced in Kg.
η_{bat}	The battery's efficiency is measured in %.
Nc	The total number of electrolyzer series cells.
n_F	Faraday efficiency.
η_{HKT}	Overall productiveness of the hydrokinetic turbine and generator.
$P_b\ (t)$	Battery's load power in kW.
ρ	The density of air in kg/m^3.
ρ_0	Air density is 1.225 kg/m^3 at sea level under normal conditions.
$P_{OUT,STP}$	Wind turbine output in kW at STP.
P_{rotor}	The rotor produces a specific amount of power in kW.
$P_{avaiable}$	The free stream's power capacity is measured in kW.
ρ_{water}	Water density in kg/m^3.
P_{OUT}	The power output of a wind turbine in kW.
$R_{n,hydrogen}$	Normal hydrogen mass flow in kg/H.
$R_{Pro.}$	Project lifetime in years.
S	Equipment number.
$	United state doller (USD).
v_{Water}	Water flow speed in m/s.
V_{bus}	The voltage in the bus.
WT_{Hight}	The wind turbine height speed is in m/s.
WT_{wsm}	Meter height wind speed measurement in m/s.
Y_{spv}	The PV array's rated capacity in kW.
Z_{height}	The wind turbine's height is in meters.
$Z_{Surface}$	The surface roughness length is measured in meters.
Z_{wsm}	The height of the wind speed is measured in meters.

1. Introduction

Renewable energy resources are crucial to achieving sustainable development goals (SDGs) and promoting global sustainable development. Among those, one critical goal is accessibility, which ensures affordable and clean energy (SDG-7); the three main sub-components of SDG-7 are energy accessibility, renewable energy penetration, and energy intensity for developing sustainable remote or rural communities and infrastructure (Elavarasan et al., 2023). Rural communities face significant energy challenges due to their remote locations, limited financial resources, and inadequate infrastructure. These challenges impede access to reliable, affordable, and sustainable energy sources, impacting not only energy accessibility but also the socio-economic landscape and overall development of these communities. Geographical remoteness makes extending centralized energy grids to these areas difficult and costly, leading to reliance on off-grid, standalone, or autonomous microgrid solutions (Mulenga et al., 2023).

The standalone or autonomous microgrids operate independently by integrating renewable energy sources like solar, biomass, geothermal, hydel, wind, and wave energy systems to produce electricity and hydrogen energy. The main advantages of integrating renewable energy sources include stability and reliability,

resilience, maximized energy production, energy storage solutions, reduction in environmental impact, and cost-effectiveness. DC microgrids offer several advantages: efficiency, integration with renewable energy, stability and control, cost efficiency, flexibility, and scalability (Modu et al., 2023b). An integrated solar PV/wind/hydro kinetic energy-based standalone DC microgrid system with batteries and hydrogen-based storage is the best choice to meet rural areas' load requirements, such as domestic, community, agriculture, and irrigation applications. The stored hydrogen is used for agro-farming hydrogen loads. Over the past few years, several studies have been offered for the feasibility and opto-techno-economic analysis of the microgrid structure for various types of loads across the globe.

The literature review (presented in Section 2) identifies the following research gaps:

- Most research studies focus on AC microgrids or hybrid microgrids with AC/DC converters; there is limited research on standalone DC microgrids, integrating renewable energy sources to produce green hydrogen and electricity for remote area applications.
- Limited studies address load categorization and comparisons between the different renewable energy integration scenarios of off-grid hydrogen-based energy solutions for remote area applications.
- Moreover, to the authors' best knowledge, the study of a green hydrogen-based DC microgrid integrated with solar/wind/HKT resources and categorizing the DC loads for remote area applications is not available in the literature. It may be considered a novelty of this study.

In addition, the villagers of the remote community have lived without electricity until 2023. Limited grid-connected electricity access is available starting in 2023, but it is intermittent due to the geological location. During festivals, they had to bring generators from nearby urban areas (Puppala et al., 2024; Puppala et al., 2025). The main motivation of this study is to provide clean, affordable, and uninterrupted electricity to the remote villages of Dayarthi and Rachakilam by integrating solar, wind, and hydrokinetic energy sources with battery-based, standalone, DC microgrids to produce green hydrogen and electricity. Access to uninterrupted electricity will also have a positive impact on the education, healthcare, and economic development of the remote villages. This will not only improve the quality of life for residents but also contribute to global efforts to combat climate change.

Based on the research gaps, the aim of the study needs to address the following research questions. Identifying what renewable energy sources are available in remote areas and how to integrate them? How can the loads be categorized, and what is the impact on the DC microgrid? How can a standalone DC microgrid optimally be designed for the load requirements of the remote area? What are the socio-economic benefits of the design of DC microgrids?

The study effectively addresses research gaps, objectives, and questions by addressing the following contributions.

- To propose and analyze integrating solar, wind, and hydrokinetic energy sources with battery-based, standalone, fully DC microgrids to produce green hydrogen and electricity for remote area applications.
- To evaluate a scenario-based approach for standalone solar (scenario #1), hybrid solar, wind (scenario #2), and fully integrated solar, wind, and hydrokinetic systems (scenario #3), optimal, technical, economic, and environmental perspectives.
- The study categorizes DC loads into primary load-1 (domestic loads), primary load-2 (community loads), and deferrable loads (irrigation and agriculture loads) for enhancing system resilience.
- The study evaluates the performance of three scenarios based on key evaluation parameters like net present cost (NPC), levelized cost of electricity (LCOE), and levelized cost of hydrogen (LCOH), and identifies the most feasible and cost-effective hydrogen and electricity generation scenario.
- Reliability analysis is conducted to thoroughly examine the performance indicators and optimal design

of DC microgrids. It involves considering various values for the maximum annual capacity shortage, referred to as CSF, ranging from 0% to 10%.

- This study is helpful; hydrogen gas is used for storage and farming practices like tractors, harvesters, crop drying machinery, and other farm machinery, which can be powered by hydrogen fuel cells, as well as fertilizer production industries like ammonia synthesis and also Identification of Key Challenges and Future Research Directions.
- Ultimately, the study emphasizes the need to identify specific renewable energy potential to help integrate renewable energy into the power sector, mitigate climate change, and achieve the United Nation's SDG-7 (Accessibility, which ensures affordable and clean energy) and India's panchamrit goals.

This paper structures the following section to achieve these objectives: Section 2 presents the literature review, which reviews existing, relevant research. Section 3 investigates the components of the DC microgrid architecture and mathematical modeling. Section 4 investigates community energy needs, electrical and hydrogen load profiles, and the availability of solar, wind, and hydro resources. Section 5 delves into the microgrid simulation, employing a flowchart to optimize the DC microgrid. Section 6 describes the simulation results for the investigated scenarios and compares results from technical, economical, optimal, reliable, and environmental perspectives. Section 7 provides the research article conclusions.

2. Literature Review

This section presents the literature review, which reviews existing, relevant research and the latest methods and tools for integrating renewable energy sources.

Egypt's renewable hydrogen potential in three towns (New Valley, Gulf of Suez, and Damietta) using three scenarios based on renewable energy resources (RERs) is evaluated (Al-Orabi et al., 2023b). The first scenario involved solar solid energy; the second used significant winds; and the third combined both solar and wind energies. Homer Pro software is simulated and optimized to minimize NPC, LCOE, and LCOH. A sensitivity analysis assessed the system's durability and efficiency by comparing the effects of an electrical power deficit and a change in the hydrogen load. The research examines three potential sites for green hydrogen production and analyzes their performance. The wind scenario at the Suez Gulf coast yielded the lowest LCOE (0.308 $/kWh) and COH (3.73 $/kg). Kapen et al. (2022) investigate the technical and financial viability of two different hybrid energy systems for Maroua. Solar photovoltaics, biogas, electrolyzer, and fuel cells with and without storage are all considered. The researcher's work combines an electrolyzer, fuel cell, and hydrogen tank to reduce battery storage requirements, considering low, medium, and high household electricity demands in communities. The LCOE and LCOH for low, medium, and high consumer communities were found to be 0.871$/kWh, 0.898$/kWh, 1.524$/kWh, 7.66$/kg, 4.95$/kg, and 0.45$/kg, respectively. Similarly, scenario 2: 0.139$/kWh, 0.091$/kWh, 0.071$/kWh, 0.139$/kWh, 0.091$/kWh, 0.071$/kWh, 3.06$/kg, 1.34$/kg, and 0.15$/kg. Ngouleu et al. (2023) compare optimization techniques for designing hybrid renewable energy systems in Kousseri, Cameroon. The goal is to minimize costs and increase the reliability of the system. The study evaluates four meta-heuristic algorithms and four different system configurations. The results indicate that a hybrid system comprising solar cells, wind turbines, and batteries is the most dependable and cost-effective setup. The optimal number of components and energy cost for high, medium, and minor activity levels are also provided and identified. The best design includes 19 SPV, 5 WT, 18 battery banks, and one inverter at 0.2641$/kWh LCOE. Al-Orabi et al. (2023a) examined Egypt's hydrogen storage options, examining five distinct setups spread across three locations. The first configuration used solar panels, an electrolyzer, a hydrogen fuel cell, and a hydrogen storage tank. The second configuration used wind turbines for electricity generation, while the third combined wind and solar energy. The fourth configuration used a diesel engine and wind turbine, and the

final configuration was identical. Diesel generators and alternative energy sources had their greenhouse gas emissions assessed by HOMER. The second configuration had the lowest LCOE, LCOH, and NPC, while the final configuration produced 87,021 kg of CO2 annually. Salhi et al. (2023) discussed wind-based hydrogen synthesis for fuel cell vehicle refueling and techno-economic optimization. The article compares three wind-powered hydrogen refueling stations with backup batteries, fuel cells, and grid connections. The analysis determines wind turbine, electrolyzer, power converter, and storage tank capacities based on wind potential, equipment costs, and hydrogen load. The grid-connected WP-HRS system has the lowest NPC (686,790 $) and LCOH (6.59 $/kg). This device produces 80,000 kg/year of green hydrogen.

Manoo et al. (2024) used geographical and meteorological data to optimize the equipment size for a hybrid renewable energy system with hydrogen storage on Bozcaada Island, Turkey, using HOMER. Two scenarios are considered: wind turbines alone and wind turbine/PV hybrids. Hybrid systems reduce NPC and hydrogen tank capacity, with LCOE ranging from $1.016 to $0.83/kWh. The most optimal system components are a 300 kW PV array, a 150-kW wind turbine, a 100-kW fuel cell, a 150-kW converter, a 200 kW electrolyzer, and a 400 kg hydrogen tank. Hasan et al. (2023) presented three cost-effective green hydrogen synthesis, transportation, and electricity-generating scenarios for isolated Australian islands using HOMER Pro. The study reveals that hydrogen technology can offer lower-cost electricity and reduced CO_2 emissions, with an LCOE ranging from $0.37/kWh to $1.08/kWh, depending on scenarios and critical parameters. The sensitivity analysis indicates that reducing the size of solar PV and wind and utilizing an undersea cable for electricity transfer could lower the levelized cost. Xia et al. (2021) investigated the viability of an off-grid renewable energy system, combination of solar, wind and hydrokinetic power, capable of providing electricity and hydrogen to a remote micro-community. The results showed that the net present cost, levelized cost of electricity, and levelized cost of hydrogen were $333, 0.74, 0.1155 $/kWh, and 4.59 $/kg, respectively. The study also showed that the PV system generated 43.7% of electricity, while the wind and hydrokinetic turbine developed 23.6% and 32.6%. Phurailatpam et al. (2018) examines rural and urban DC microgrid planning and optimization in India. The study reveals that autonomous microgrids incur an energy cost of $0.27 per unit. Integrating renewable generation in rural areas with partial grid connectivity allows continuous electricity for $0.163 per unit. In urban areas, biodiesel generators are considered, resulting in a cost of energy of $0.23 for residential buildings and $0.21 for IT business organizations. Energy prices fluctuate slightly depending on the availability of renewable and local energy sources.

Modu et al. (2023a) investigated wind, biomass, hydrogen, and battery-based energy systems and capacity planning of a standalone hybrid energy system with the Swarm nature-inspired metaheuristic optimization algorithm (SSA). The EMS-SSA algorithm offers the lowest levelized cost of energy of $0.939737/kWh, outperforming other algorithms like EMS-LFA, EMS-GA, and HOMER. Al-Shetwi et al. (2023) analyzed five hybrid energy systems based on renewable energy sources in Saudi Arabia, focusing on their technical compatibility, economic feasibility, and environmental implications. Irshad et al. (2023) reported a solar wind and hydropower resource-based hybrid system investigated the optimal configuration using the multi-objective genetic algorithm (MOGA) optimization technique, which has the lowest NPC, COE, and the best target capabilities for 25 years. The optimization of hydroelectric plants, wind turbines, and PV panels in Hinnoya, Norway is investigated (Hoseinzadeh et al., 2023). The study finds that using renewable energy systems leads to lower electricity generation costs, with LCOE production at least 50% lower than the grid's average prices. Onshore wind turbines have more potential than offshore ones. Using renewable systems in households can reduce LCOE by nearly 70%, as well as in transportation and industrial fields by 50%.

Table 1. Literature review on the feasibilities of integrated renewable microgrids.

References	Location	Renewable energy recourses				Storage		DC loads	Operation mode	method	LCOE ($/kwh)	LCOH ($/kg)	Capacity shortage effect
		SPV	Wind	HKT	Bio gas	BAT	HT						
Al-Orabi et al. (2023b)	Egypt	√	√	X	X	√	√	X	Off-grid	HOMER	0.308	3.73	X
Kapen et al. (2022)	Maroua	√	X	X	√	X	√	X	Off-grid	HOMER	0.35	7.66	X
Ngouleu et al. (2023)	Cameroon	√	√	X	X	√	X	X	Off-grid	MHO	0.2641	X	X
Al-Orabi et al. (2023a)	Egypt	√	√	X	X	√	√	X	Off-grid	HOMER	0.308	3.96	X
Salhi et al. (2023)	Oman	X	√	X	X	√	√	X	Off-grid	HOMER	X	6.79	X
Manoo et al. (2024)	Pakistan	√	√	X	X	√	√	X	Off-grid	HOMER	0.37	X	X
Hasan et al. (2023)	Australia	√	√	X	X	√	√	X	Off-grid	HOMER	0.25	X	X
Xia et al. (2021)	Iran	√	√	√	X	√	√	X	Off-grid	HOMER	0.1155	4.59	X
Phurailatpam et al. (2018)	India	√	√	X	X	√	X	√	Off-grid	HOMER	0.27	X	X
Modu et al. (2023a)	Nigeria	√	√	X	√	√	√	X	Off-grid	SSA	0.93	X	X
Al-Shetwi et al. (2023)	Saudi Arabia	√	√	X	X	√	√	X	On-grid	HOMER	0.048	X	X
Irshad et al. (2023)	Kandahar	√	√	X	X	√	X	X	Off-grid	MOGA	0.35	X	X
Hoseinzadeh et al. (2023)	Norway	√	√	X	X	√	X	X	On-grid	HOMER	0.055	X	X
Vakili and Ölçer (2023)	Philippines	√	√	X	X	√	X	X	On-grid	HOMER	0.081	X	X
Zeyad et al. (2023)	Dhaka	√	√	X	√	√	X	X	On-grid	HOMER	0.035	X	X
Amoussou et al. (2023)	Spain	√	X	X	X	√	X	√	Off-grid	SAM	0.95	X	X
Bakeer et al. (2023)	Marsa Matruh	√	√	X	X	√	X	X	Off-grid	AVOA	0.094	X	X
Al-Ghussain et al. (2022)	Jordon	√	√	X	X	√	√	X	On-grid	HOMER	0.065	2.03	X
Turkdogan et al. (2021)	Turkey	√	√	X	X	√	√	X	On-grid	HOMER	0.038	3.54	X
Jahangiri et al. (2019)	Chad	√	√	X	X	√	√	X	Off-grid	HOMER	0.39	21.5	X
Jahangiri and Nowdeh (2020)	Iran	√	√	X	X	√	√	X	Off-grid	SCA, PSO	0.76	5.4	X
Das et al. (2024)	India	√	√	X	X	√	√	X	Off-grid	HOMER	0.252	2.59	X
Yadav et al. (2024)	India	√	√	X	X	√	√	X	Off-grid	HOMER	0.232	36.6	X
Alluraiah and Vijayapriya (2023)	India	√	√	X	X	√	√	X	On-grid	HOMER	0.78	20.7	X
Praveenkumar et al. (2022)	India	√	X	X	X	√	√	X	Off-grid	HOMER	0.41	3.22	X
Present	**India**	√	√	√	**X**	√	√	√	**Off-grid**	**HOMER**	**0.197**	**3.98**	√

SPV, Solar Photovoltaic; HKT, Hydrokinetic Turbine BAT, Batteries; HT, Hydrogen tank; MHO, Meta-Heuristics Optimization: SSA, Salp Swarm nature-inspired metaheuristic optimization algorithm; SAM, System Advisor Model; AVOA, African Vultures Optimization Approach; SCA, Sine–Cosine Algorithm; PSO, Particle Swarm Optimization; HOMER, Hybrid Optimization Model for Electric Renewables;

A study on the Philippines' domestic ferries (Vakili and Ölçer, 2023) found that solar and wind power systems are cost-effective and environmentally friendly, and switching from diesel to gas generators reduces operating costs. The author suggests a design for a community microgrid in Hazaribagh, Dhaka, which employs photovoltaic installations on rooftops to curb pollution and greenhouse gases, thereby providing a 52% reduction in energy expenses (Zeyad et al., 2023). The researchers in (Amoussou et al., 2023) wanted to build a hybrid photovoltaic and wind power plant in Limbe, southwest Cameroon, to replace a heavy-fuel oil thermal power plant. They wanted to do this while keeping the total cost as low as possible and making the most of Moth Flame Optimization (MFO), Improved Grey Wolf Optimizer (I-GWO), Multi-Verse Optimizer (MVO), and the African Vulture Optimization Algorithm (AVOA). The African Vulture Optimization Approach (AVOA) is used to run a microgrid in Marsa Matruh, Egypt, that is self-sufficient and uses a mix of renewable energy sources. This method gets better economic results with the lowest net present cost and energy price (Bakeer et al., 2023). Jordan utilizes excess energy from large-scale renewable energy systems for co-generation, particularly wind-based systems with a high demand-supply ratio and a low hydrogen cost (Al-Ghussain et al., 2022).

A hybrid energy system for a single-family house that could meet utility and transportation needs is explored (Turkdogan, 2021), where the system-levelized electricity and hydrogen production costs are 0.685$/kWh and 6.85$/kg, respectively. A solar-wind hybrid system is a cost-effective solution for addressing the energy gap in remote towns in Chad is reported (Jahangiri et al., 2019). Using hydrogen, the system can generate electricity and store surplus power. For the studied stations, the average total NPC was $48,164, and the average LCOE was $0.573. The Recreational Center of Gonbad (RCOG) in Iran found that a hybrid photovoltaic/wind/fuel cell system, optimized using the improved sine-cosine algorithm (ISCA), is the most cost-effective option proposed in Jahangiri and Nowdeh (2020). Das et al. (2024), a decentralized hybrid energy system, precisely the solar-wind-diesel-battery electrolyzer combination, is the optimal solution for sustainable electricity and hydrogen production. This system meets the required load, produces hydrogen as a by-product, and has the lowest cost and best environmental impact. The renewable share of this system is 98.4%, with a payback period of 6.1 years. The estimated costs are $0.252/kWh for electricity and $2.59/kg for hydrogen. The sustainability assessments were evaluated using a multi-criteria decision-making approach.

A hybrid renewable energy source (RES) with a multiple-ESS system, utilizing HOMER for optimal design and energy consumption (Yadav et al., 2024), ensures low NPC and LCOE during capacity shortages. (Alluraiah and Vijayapriya, 2023), a hybrid microgrid system utilizing renewable energy sources is proposed for Doddipalli village, Chittoor, India. The system includes a hydrogen tank, is energy-efficient, and is cost-effective, with a LCOE of $ 0.0751/kWh/d, a minimum NPC of $ 6.92M, and a high renewable energy fraction of 97.8%. (Praveenkumar et al., 2022), the study concludes that solar-powered PV modules have the potential to support the technical, economic, and environmental viability of hydrogen production projects in five Indian cities. The study found that Kolkata had the highest hydrogen production, followed by Chennai, Ludhiana, Indore, and Mumbai. This highlights the potential of hydrogen production in India. The above literature is summarized based on the feasibility of integrated renewable microgrids in **Table 1.** It is evident that the optimal, technical, economic, and reliability analysis on renewable energy systems integrated with solar photovoltaic panels, wind turbines, biogas with batteries, and hydrogen storage are available at different geographical regions, where the optimal cost of hybrid systems varies by geographical region, indicating that the economic profitability of these systems is site-specific rather than the method's superiority or deficiency.

3. Proposed Microgrid Architecture and Components

The proposed DC microgrid schematic diagram in **Figure 1** includes various renewable energy resources and storage components. The primary integrated renewable energy resources commonly connected to the DC bus are solar PV panels, wind turbines, and hydrokinetics. The DC bus serves the electrical loads, including DC primary and deferrable loads, with a battery backup. When there is a shortage of renewable energy resources, the battery provides electricity to the loads. Additionally, the electrolyzer connects to the DC bus, converting the DC electric supply into hydrogen gas, which the hydrogen tank then delivers to the hydrogen load. The proposed DC microgrid system offers a sustainable and reliable solution for both captive electrical and hydrogen loads while maximizing the utilization of renewable energy resources.

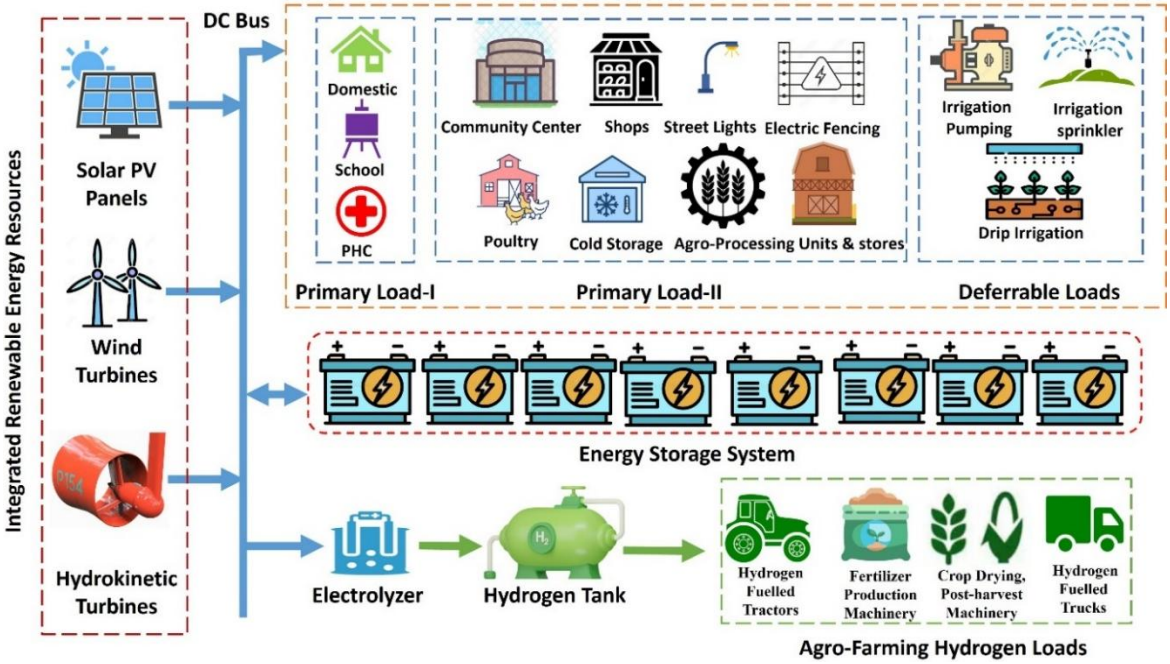

Figure 1. Proposed DC microgrid schematic diagram.

3.1 DC Microgrid Components Analysis

The DC microgrid system consists of various essential components, including solar PV panels, wind turbines, hydrokinetic turbines, batteries, an electrolyzer, and a hydrogen tank. The mathematical model of the components is as follows.

3.1.1 Solar PV Panels

Solar PV modules convert solar radiation into a direct current of electricity. These modules can be connected in series or parallel to form strings or PV arrays. Using series or parallel connections in a PV energy system depends on the desired voltage and current requirements. By combining multiple strings or arrays, the overall power output can be further increased. Homer (2024) describes the calculation for the output power of the solar PV panel in Equation (1). The solar panels have an installed cost of $400 per kilowatt (kW) and do not require any replacement costs within their 25-year lifespan. The cost of operating and maintaining the panels (O&M) is 5 $ per kW per year (Elmorshedy et al., 2022).

$$P_{SPV} = Y_{SPV} * F_{SPV} \left(\frac{G_T}{G_{T,stc}}\right) \quad (1)$$

3.1.2 Wind Turbine

The wind energy generation is modeled using a generic 10 kW wind turbine available in the HOMER library. The power output of a wind turbine is calculated using the power curve, which involves determining the wind speed at the hub height using user inputs from wind resources. The power output is then determined using the power curve at the calculated wind speed. Finally, the power output value is adjusted for the actual air density. The wind turbine model and the output power are as follows (Homer, 2024), in Equation (2).

$$WT_{Hight} = WT_{wsm} * \frac{ln\left(\frac{Z_{height}}{Z_{Surface}}\right)}{ln\left(\frac{Z_{wsm}}{Z_{surface}}\right)} \quad (2)$$

The output power is in Equation (3) determined by multiplying the air density ratio with a specific formula, as stated in reference (Homer, 2024), while considering the current conditions.

$$P_{OUT} = \left(\frac{\rho}{\rho_0}\right) * P_{OUT,STP} \quad (3)$$

A 10-kW wind turbine is selected based on the load requirements. **Figure 2** represents the power curve for the turbine, and it has a hub height of 24 m. Elmorshedy et al. (2022), the total cost of installing the turbine is 11,000 $ per turbine, and there is no replacement cost as the turbine has a lifespan of 25 years, which matches the project's duration. The operation and maintenance costs are 30 $/kW/year.

3.1.3 Hydrokinetic Turbine Model

Hydrokinetic turbines transform water's kinetic energy into mechanical energy, thereby producing electricity. **Figure 3** represents the power output of a turbine increases significantly as water speed increases. However, there is a point where the power output levels off and may even decrease at extremely high speeds. The turbine operates at its highest efficiency, effectively converting the kinetic energy of flowing water into electrical power. Equation (4) and Equation (5) are used to calculate the amount of energy generated by this type of turbine (Noruzi et al., 2015; Vermaak et al., 2014).

$$E_{HKT} = 0.5 * \rho_{water} * A_{HKT} * (v_{wATER})^3 * C_{\rho HKT} * \eta_{HKT} * h \quad (4)$$

which can be obtained by Equation (5) (Vermaak et al., 2014).

$$C_{\rho HKT} = \frac{P_{rotor}}{P_{avaiable}} \quad (5)$$

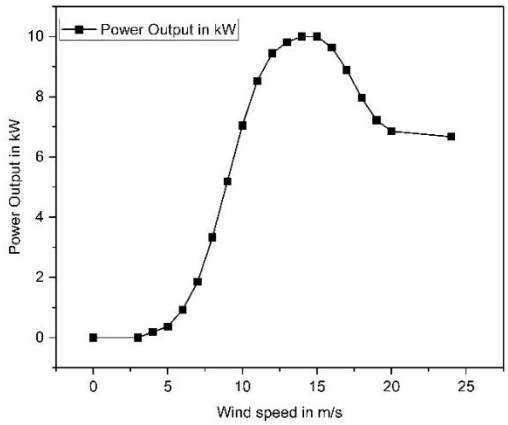

Figure 2. Power curve of the wind turbine.

A 20-kW hydrokinetic turbine with an initial cost of 35,000 $, replacement and operating costs of 21,000 $ and 1200 $ per year, and a life expectancy of 25 years.

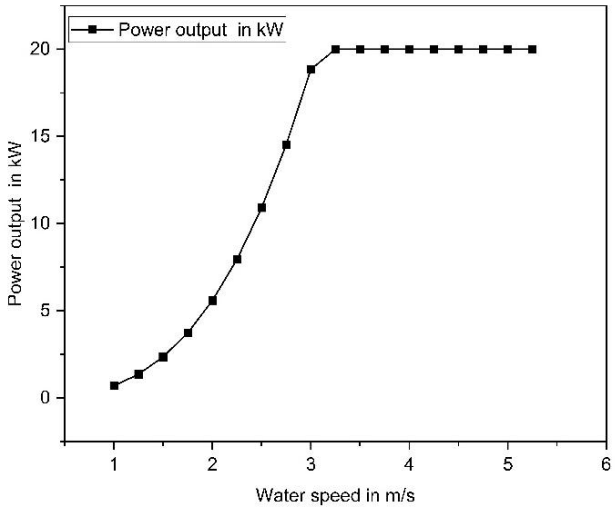

Figure 3. Power curve of hydrokinetic turbine.

3.1.4 Battery

Battery systems are crucial for power generation reliability, storing surplus electricity to supply energy during energy shortages. In a microgrid, batteries charge during sunny hours, and excess energy is available to compensate for intermittent energy when sources are unavailable. Equation (6), Cano et al. (2020) determine the state of charge. The proposed DC microgrid uses a generic 100kWh Li-Ion, which has an initial cost of $12,000, replacement costs of $12,000 and $20, and a life expectancy of 20 years.

$$SOC(t) = SOC(t-1) * \int_{t-1}^{t} \frac{P_b(t) * \eta_{bat}}{V_{bus}} \, dt \quad (6)$$

3.1.5 Electrolyzer and Hydrogen

The electrolyzer is a device that uses a direct current to split water (H2O) or other electrolyte solutions into hydrogen (H_2) and oxygen (O_2). The electrolyzer harnesses the excess electricity from renewable energy sources to generate hydrogen, subsequently storing it in a hydrogen tank. The rate of hydrogen obtained should be determined using Equations (7), and the electrolyzer energy requirement calculated in Equation (8) (Al-Orabi et al., 2023b; Rad et al., 2020). Uninstalled electrolyzer have a capital cost of 460 $/kW, with installation accounting for 12% of the cost. The total cost is $516/kW, with OPEX at 2% per year. The lifetime stack replacement cost is $260/kW (Al-Orabi et al., 2023b).

$$R_{hydrogen} = \frac{I_{ele} * n_F * N_c}{2F} \quad (7)$$

$$E_{ele} = B_E * R_{n,hydrogen} + A_E * R_{hydrogen} \quad (8)$$

3.1.6 Hydrogen Tank

During electrolysis, the generated hydrogen gas is stored in the hydrogen tanks. A hydrogen tank stores hydrogen gas for various applications, including energy storage, renewable energy integration, and backup power systems. In the present article, hydrogen gas is used for different farming applications. Using stored hydrogen gas in farming applications offers numerous benefits, including enhanced agricultural practices,

reduced dependence on traditional energy sources, and promoting sustainable and environmentally friendly farming practices. The tank's lifetime is 25 years, with a capital cost of $200/kg, a replacement cost of $200/kg, and a zero-operating cost.

4. Study Area, Load Profile, and Resources

Due to the significant investment costs and location associated with constructing the utility grid, remote villages usually need to connect to the grid infrastructure. The electricity of such remote villages may be possible through microgrids by integrating renewable energy sources. Consider the case study in the current work on one of these communities in a remote rural area of Andhra Pradesh (India). Alluri Sitharama Raju district, centered in Paderu, is one of six districts in the North Coastal area of the Indian state of Andhra Pradesh. According to the district's physical features data from the state, the Eastern Ghats provide a natural backdrop for the exquisitely beautiful district that bears the region's name. As per the district's demographic and literacy data, the district had a total population of 953,960 as of the 2011 census, of which only 37,973 (3.98%) lived in urban areas, while the rest, 915,987 (96.02%), lived in rural areas. The district also had a literacy rate of 42.34%. This district proposes the villages of Dayarti and Rachakilam as the case study locations for the suggested methodology. The remote villages of Dayarti and Rachakilam have good solar and wind resources; good hydrokinetic resources are also available. As per the district's demographic and literacy data, Dayarthi and Rachakilam have a total geographical area of 131 hectares and a population of 461 people. There are a total of 96 homes in the two villages. The average literacy rate of these villages is 20.34%. The grid extension is not most suitable for these remote and hilly villages. There is a possibility of establishing an autonomous DC microgrid in remote villages (18.0391° N and 82.9159° E).

Electrical loads throughout the villages are divided into three main groups. Like primary load-1, primary load-2, and deferrable loads shown in **Table 2**, primary load-1 includes 96 homes for domestic needs, a primary school, and a village health clinic. Primary load-2 includes the community center, street lights, and small agriculture support units. **Figure 4** shows the graph, which displays the average primary load of 1 and 2 hourly profiles. For this microgrid setup, deferrable loads like irrigation pumping, irrigation sprinkler systems, and drip irrigation systems are also used. The deferrable load is taken to utilize a storage capacity of 56 kW. The total demand for electrical power in the village is an average of 498.74 kW/h.

Both agricultural machinery and farming applications use hydrogen fuel simultaneously. The average requirement for fuel for farm machinery (tractors), crop drying machinery, fertilizer production machinery, post-harvest handling machinery, and agricultural product transportation (hydrogen-powered trucks) is 25 kg/day. **Figure 5** displays the average peak load demand of primary loads, deferrable loads, and hydrogen loads, and **Figure 6** shows the average hourly load profile for hydrogen.

The national renewable energy database is used by the Homer simulation method to provide resource data like temperature, solar irradiation, and wind speed that can be used to make realistic microgrid models. As per the data provided by the state irrigation department, Raiwada Reservoir (82° 59' 00" E and 13° 00' 30" N) is a medium-type reservoir that was constructed across the River Sarada near Devarapally village to provide irrigation to an extent of 21,344 acres in Visakhapatnam District and Vizianagaram District. Besides, 50 cusecs of water are allocated to serve the drinking water needs of Visakhapatnam city by suppressing 6,000 acres of ayacut in Vepada, Kotapadu, and Devarapalli Manda. As per the data provided by the state irrigation department, the gross capacity at the full reservoir level (FRL) is 3.6 thousand million cubic feet (TMC), the average storage is 3.2 TMC, the current storage is 0.92 TMC, the average inflow is 125 Cusecs, and the outflow is 125.81 Cusecs. It is feasible to place hydrokinetic turbines in the Saradha River to generate electric energy (Dandupati et al, 2024).

Solar irradiation, clearness index, and temperature play an important role in the output of solar PV panels. **Figure 7** shows the daily solar irradiation for each month. It observes that irradiance is high in April and May due to the high temperature; the average irradiance is 5.13 kWh/m^2/day. **Figure 8** represents the average wind speed. In July, the wind speed is higher, and the average wind speed is 5.53 m/s. Similarly, **Figure 9** represents the hydrokinetic turbine water velocity; it is considered that the average water velocity of each month shows in August and September, the water speed is higher; the annual average is 2.52 m/s.

Table 2. The division of electrical loads throughout the village.

S. No.	Consumer	Appliance	Power (W)	Quantity	Total power (W)	Hrs./Day	Energy (kWh)/Day
1.	Primary load-1 (Domestic loads)	Lighting bulbs	15	4	60	5	0.3
		Security bulb	15	1	15	11	0.165
		Ceiling fans	40	2	80	8	0.64
		Radio	20	1	20	8	0.16
		Charging devices	50	1	50	2	0.1
		Load for one house	140	9	225	34	1.365
		Total load for 96 houses	1.365 x 96				131.04
		Primary health centers	500	2	1000	11	11
		School	600	1	600	9	5.4
		Total primary load-1 (Domestic loads)					**147.44**
2.	Primary load-2 (Community loads)	Community center	400	1	400	4	1.6
		Street lights	60	50	3000	12	36
		Agro-processing units	2000	4	8000	12	96
		Agricultural supply stores	500	6	3000	4	12
		Poultry and livestock housing	400	2	800	24	19.2
		Cold storage	3000	1	3000	24	72
		Electric fencing to protect crops	500	1	500	11	5.5
		Total primary load-2 (Community loads)					**242.3**
3.	Deferrable loads (Agriculture loads)	Irrigation pumping	5000	4	20000	5	100
		Irrigation sprinkler systems	750	2	1500	3	4.5
		Drip irrigation systems	750	2	1500	3	4.5
		Total deferrable loads (Agriculture loads)					**109**
Total Primary and deferrable load							**498.74**

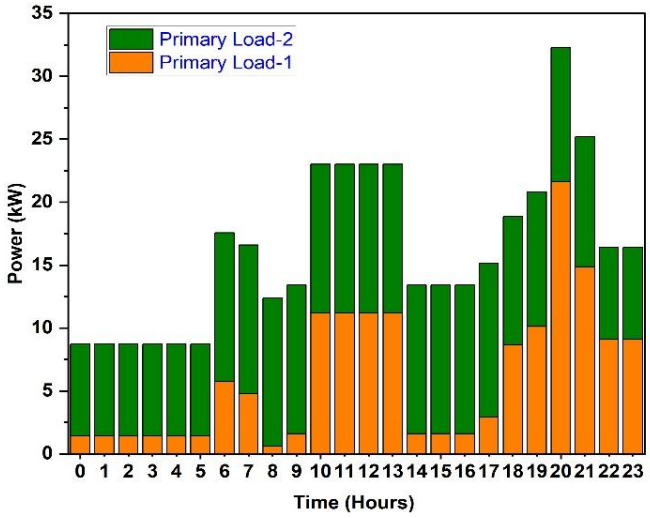

Figure 4. Average primary load 1 and 2 hourly profile.

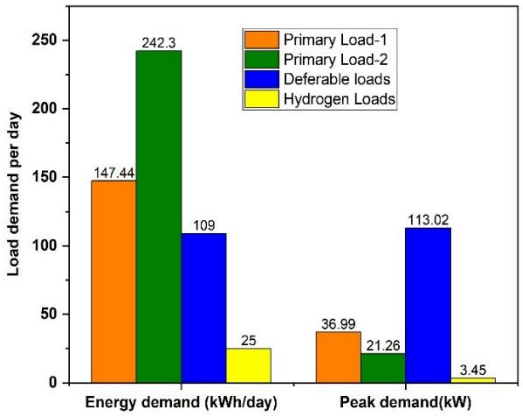

Figure 5. Energy demand and peak demand per day.

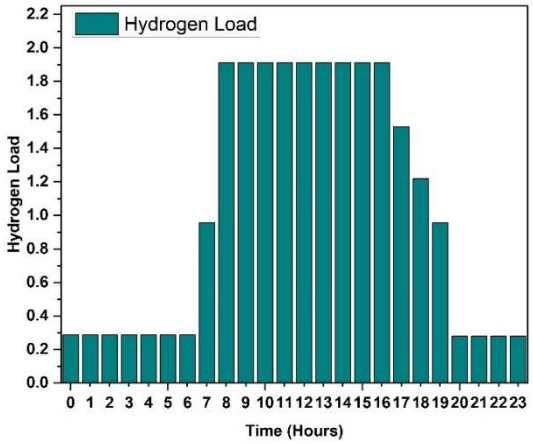

Figure 6. Hydrogen loads average hourly load profile.

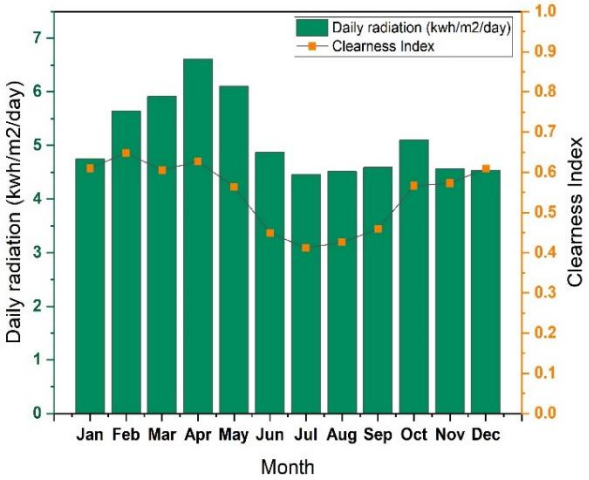

Figure 7. Average monthly solar irradiation.

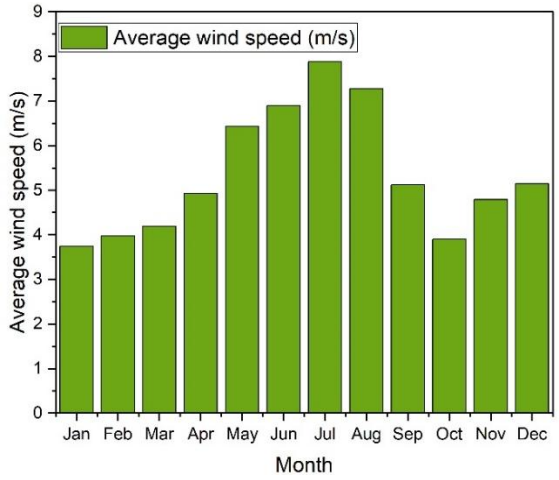

Figure 8. Average monthly wind speed.

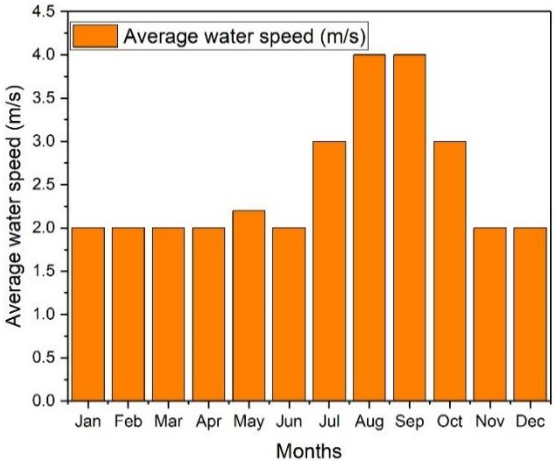

Figure 9. Average monthly water velocity and output.

5. Research Methodology and Optimization Algorithm

Opto-techno economic analysis for the proposed DC microgrid architecture is performed using Homer Pro software version 3.16.2 on a laptop with the following specifications: 11th Gen Intel (R) Core (TM) i5-11300H @ 3.10GHz and 16.0 GB of RAM (Puppala et al., 2025). Simulating a system configuration evaluates its technical viability and life-cycle cost. The optimization approach affects several system configurations to find one that meets technical limitations at the lowest life cycle cost. The total NPC, LCOE, and LCOH are the primary economic factors in the optimization process. The NPC is the sum of the component's overall lifecycle costs, including installation and operation, minus the revenue generated by the project. The NPC reduces expected future expenditures and income by discounting them to their present value. The economic value added by the component to the project is determined. Similarly, LCOE and LCOH are the ratios of the total annualized cost to the energy served by the electrical and hydrogen loads. The total NPC, LCOE, and LCOH are calculated from Equation (9) to Equation (17) below.

Min [CNPC, Pro. LCOE, LCOH] (9)

$$C_{NPC,Pro.} = \sum_{s=1}^{J} [C_{NPC,Tot.,Eq.}]_s \quad (10)$$

$$C_{NPC,Tot.,Eq.} = \sum_{m=0}^{m}[C_{tot.,Eq.m} * d_f] \quad (11)$$

$$C_{Tot.,Eq.,m} = C_{Ear.,Eq.,m} - C_{Sp.,Eq.,m} \quad (12)$$

$$d_f = \frac{1}{(1+i)^m} \quad (13)$$

$$LCOE = \frac{C_{Tot.,Anu.}}{E_{Served}} \quad (14)$$

$$LCOH = \frac{C_{Tot.,Anu.}}{M_{Hydrogen}} \quad (15)$$

$$C_{Tot.,Anu.} = CRF(i, R_{Pro.}) * (C_{NPC,Tot.,Eq.}) \quad (16)$$

$$CRF\ (i,m) = \frac{i(1+i)^m}{(1+i)^m - 1} \quad (17)$$

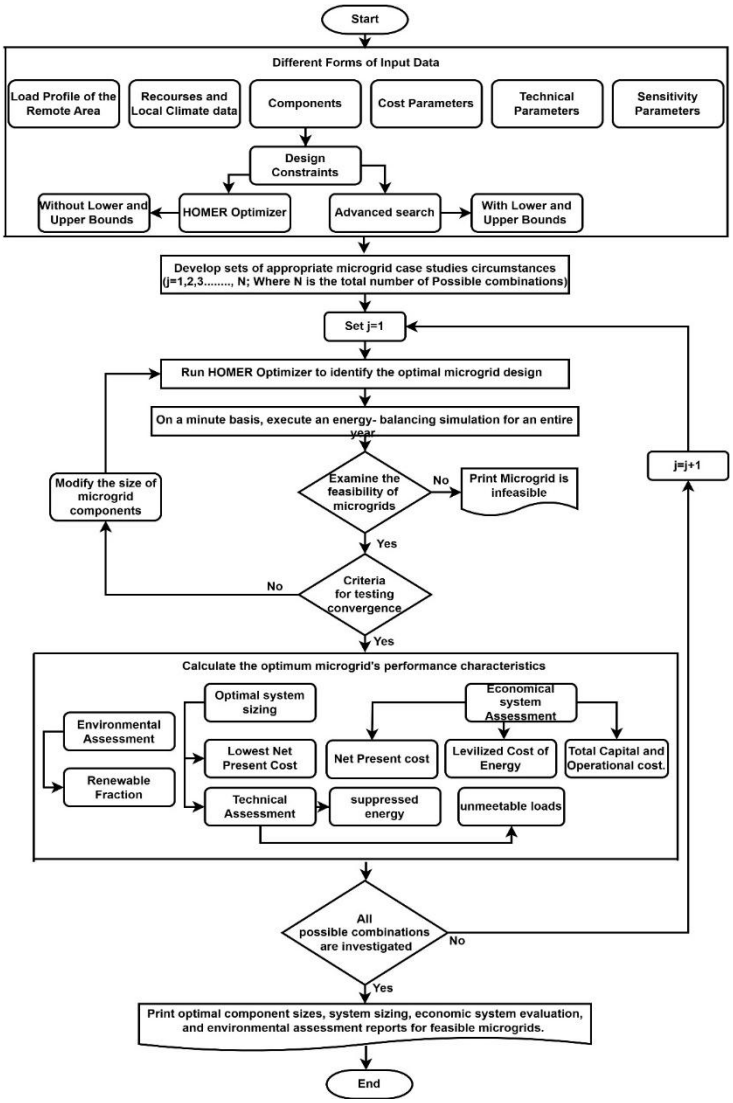

Figure 10. Applied flowchart for DC microgrid optimization (Puppala et al., 2025).

The optimization process used actual renewable potential, primary load-1, primary load-2, deferrable, and hydrogen load data. **Figure 10** displays a flowchart for microgrid optimization and the feasibility of purely renewable sources. The first step in the process is to carry out a pre-feasibility analysis of the load profile of the remote area, resources, local climate data, cost parameters, technical parameters, sensitivity parameters, and design constraint components based on the upper and lower limits. Then, on a one-minute basis, an energy-balancing simulation will be executed for an entire year. Based on the input, the optimization algorithm aims to minimize the net present cost by adjusting the decision variables such as photovoltaic array size, wind turbine number, battery capacity, electrolyzer rating, and hydrogen tank capacity. The algorithm ranks feasible solutions based on economic performance after achieving precision convergence and analyzing all possible configurations. The microgrid design employs a load-following energy dispatch algorithm, prioritizing renewable energy sources (Brown et al., 2024; Veilleux et al., 2020).

6. Results and Discussions

The section's primary focus is to analyze and compare configurations, as well as evaluate how various system components can contribute to achieving net-zero emissions and minimizing NPC, LCOE, and LCOH. The base scenario for all configurations is 147.44 kWh, 242.3 kWh, 109 kWh for DC electrical primary load-1, primary load-2, and deferrable loads, and 25 kg/day for hydrogen load, with 25 years of project life; it employs an 8% discount rate, no capacity shortage, and 0% operating reserve. **Figure 11** represents the scenarios' simulation diagrams in the following manner: Scenario #1: Solar PV/Battery/ Electrolyzer/Hydrogen Tank; Scenario #2: Solar PV /Battery/Wind Turbine/Electrolyzer/Hydrogen Tank; Scenario #3: Solar PV/Wind Turbine/Hydrokinetic Turbine /Battery/Electrolyzer/Hydrogen Tank. The DC microgrid component's specification and statistics for three scenarios are shown in **Table 3.**

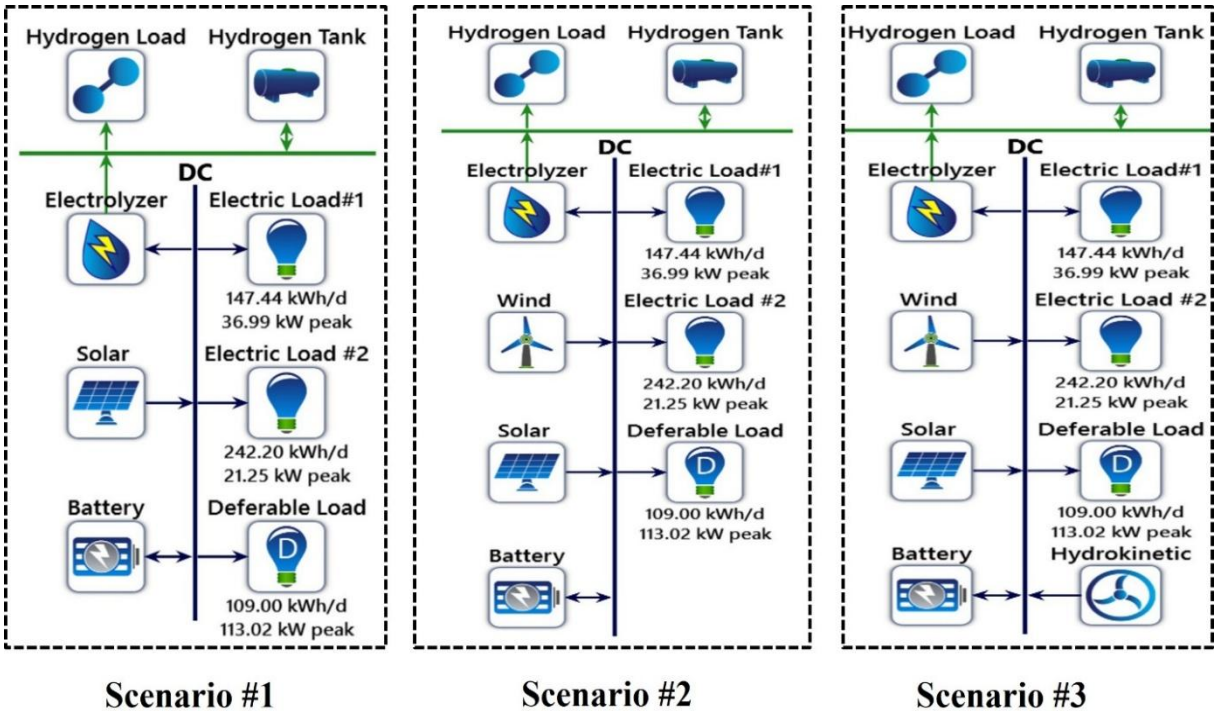

Figure 11. Simulation diagrams of three proposed microgrid scenarios.

6.1 Solar PV/Battery/Electrolyzer/Hydrogen Tank (Scenario #1)

In this DC microgrid scenario #1, four components are used: solar PV, batteries, an electrolyzer, and a hydrogen tank. The component cost summary and optimization results are in **Table 4**. It is observed that solar PV has the highest capital cost, approximately 44% of the total system cost, followed by the electrolyzer (18.7%), battery unit (10%), and hydrogen tank (7.25%). The battery has the highest replacement costs, followed by the electrolyzer and other components. Solar PV has the highest operational and maintenance costs, followed by the electrolyzer and battery. The remaining power system components salvage value following the project. **Figure 12** represents the cash flow of microgrid scenario #1 by component type in each year. The total NPC, the LCOE, and the LCOH all include the cost of solar PV, making it the most expensive source.

As seen in **Figure 13**, solar PV provided the entire year's sufficient supply of the load's energy needs. It may produce more energy in February, March, and April due to the increased solar irradiance and atmospheric conditions. A total of 608 kW is the nominal capacity of the solar PV system. **Figure 14** represents the annual energy production summary of generation sources serves the hydrogen load. The electrolyzer can produce up to 200 kW of power. The total annual output is 9,212 kg. The power input into the electrolyzer is highest during the day. A 200-kg capacity was chosen for the hydrogen tank. The heat map of annual production in **Figure 15** shows that this system generates 957,745 kWh annually, primarily between 8:00 a.m. and 4:00 p.m. The LCOE for solar PV is $0.0228/kW. The battery unit plays a significant role in an autonomous system with intermittent power sources. The all-component specifications and statistics for scenario #1 are shown in **Table 3.** It provides data on the 500-kW lead-acid battery's various statistics, including the storage wear cost of 0.0422 $/kWh. **Figure 16** represents the battery unit's annual state of charge; observe that it has an excellent percentage of the state of charge during the daytime due to the availability of solar energy, and its estimated lifespan, based on the frequency with which it would be used, is roughly 15 years. The microgrid has a daily need of 25 kg and an hourly peak demand of 3.449 kg of hydrogen gas. **Figure 17** illustrates the hydrogen tank's autonomy during the project's life cycle. It shows the overall cost of producing green hydrogen, including the LCOH of 4.63 $ per kilogram, the hydrogen load, and the hydrogen tank, and the LCOE of 0.234 $ per kWh is calculated.

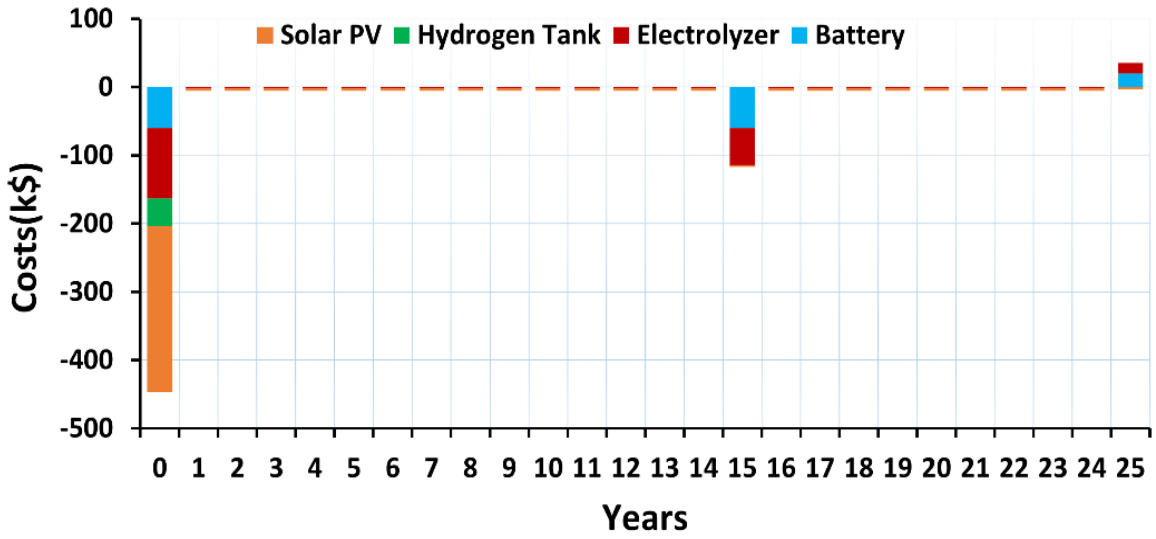

Figure 12. Cash flow of the microgrid scenario #1 by component type.

Table 3. DC microgrid component's specification and statistics for three scenarios.

Parameters	Specification	Scenario #3	Scenario #2	Scenario #1	Units
Components size	Solar PV	32	417	608	kW
	Wind turbine	20	40	---	kW
	hydrokinetic turbine	20	---	---	kW
	Battery	300	400	500	kWh
	Electrolyzer	200	200	200	kW
	Hydrogen tank	200	200	20	kg
Production	Solar PV	508,600	655,982	957,745	kWh/Yr
	Wind turbine	37,453	74,906	---	kWh/Yr
	hydrokinetic turbine	90,926	---	---	kWh/Yr
Consumption	DC primary load	142,199	142,179	142,188	Wh/Yr
	Deferrable load	39,753	39,755	39,753	Wh/Yr
	Total	600,824	421,604	427,493	Wh/Yr
Excess	Electricity	32,542	120,737	339,062	Wh/Yr
Solar PV power output data	Production	508,600	655,982	957,745	kWh/yr
	Levelized cost	0.0228	0.0228	0.0228	$/kWh
	Operation hours	4,346	4,346	4,346	hrs/yr
	Capacity factor	18	18	18	%
	Maximum output	318	410	598	kW
	Rated capacity	323	417	608	kW
Wind power output data	Production	37,453	74,906	---	kWh/yr
	Levelized cost	0.0534	0.0534	---	$/kWh
	Operation hours	7,331	7,331	---	hrs/yr
	Capacity factor	21.4	21.4	---	%
	Maximum output	20	40	---	kW
	Rated capacity	20	40	---	kW
HKT power output data	Production	90,926	---	---	kWh/yr
	Levelized cost	0.0444	---	---	$/kWh
	Operation hours	8,760	---	---	hrs/yr
	Capacity factor	51.9	---	---	%
	Maximum output	20	---	---	kW
	Rated capacity	20	---	---	kW
Battery's various statistics	Energy input	37,102	67,365	94,000	kWh/yr
	Energy output	33,488	60,752	84,751	kWh/yr
	Losses	3,715	6,743	9,408	kWh/yr
	Consumption of reserves	102	130	159	kWh/yr
	Annual throughput	35,300	64,038	89,335	kWh/yr
	Expected life	15	15	15	yr
	Autonomy	11.6	15.4	19	hr
	Cost of storage wear	0.0422	0.0422	0.0422	$/kWh
Statistics of the electrolyzer	Maximum input	200	48.1	200	kW
	Energy input	418,872	421,604	427,493	kWh/yr
	Capability ratio	23.9	24.1	24.4	%
	Operation hours	4,315	3,604	3251	hr/yr
	Maximal productivity	4.31	4.3	4.31	kg/hr
	The total output	9,026	9,085	9212	kg/yr
	Particular usage	46.4	46.4	46.4	kWh/kg
Statistics of the hydrogen tank	Hydrogen storage capacity	200	200	200	kg
	LCOH	3.98	4.24	4.63	$/kg
	Tank autonomy	321	321	321	hr
	Energy storage capacity	6,667	6,667	6667	kWh
	Storage at the beginning of the year	100	100	100	kg
	Storage at end of year	9.95	67.8	193	kg

Table 4. Component cost summary and optimization result of scenario #1.

Component	Capital	Replace	O & M	Salvage	Total
Solar PV	$243,263	$0.00	$39,310	$0.00	$282,572
Battery	$60,000	$25,456	$1,293	-$4,791	$81,958
Electrolyzer	$103,200	$22,062	$25,855	-$4,152	$146,965
HT	$40,000	$0.00	$0.00	$0.00	$40,000
Total	**$446,463**	**$47,519**	**$66,458**	**-$8,943**	**$551,495**

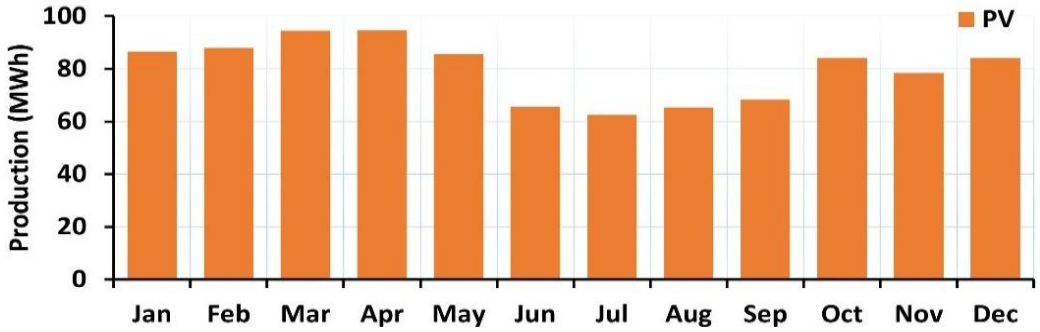

Figure 13. Annual energy production summary of standalone solar PV for scenario #1.

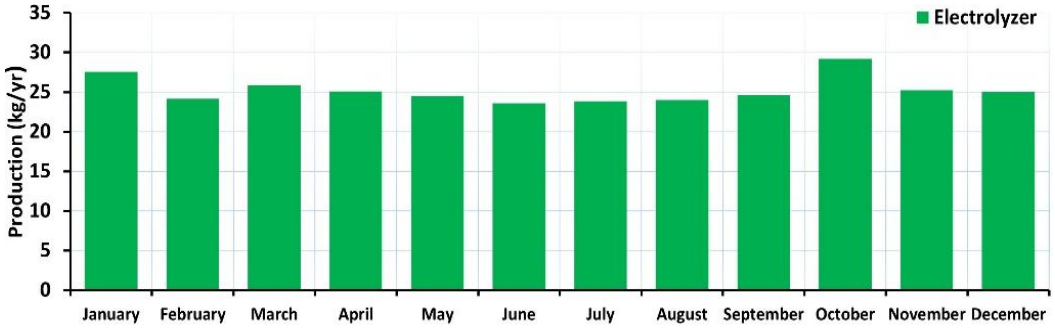

Figure 14. Annual energy production summary of electrolyzer for scenario #1.

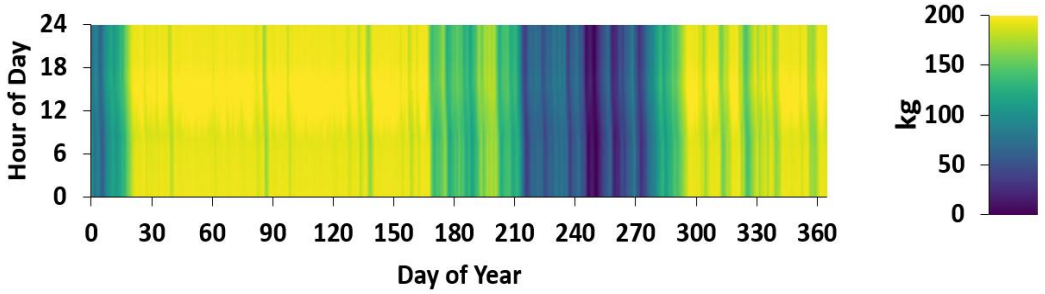

Figure 15. Annual solar production heat map for scenario #1.

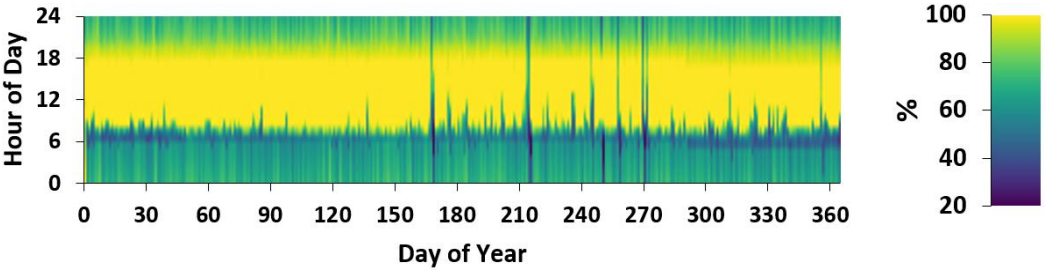

Figure 16. Annual state of charge of the battery unit heat map for scenario #1.

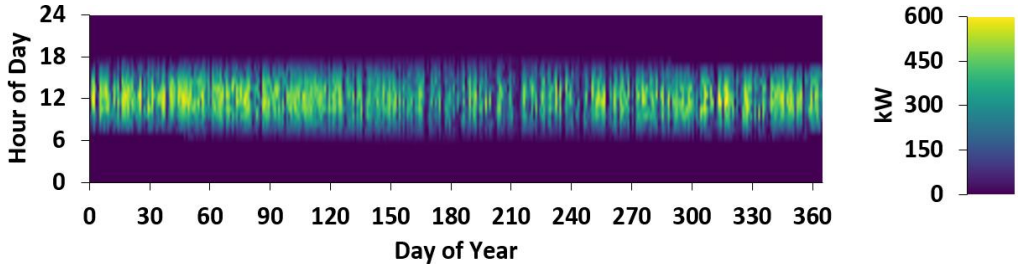

Figure 17. Annual hydrogen tank autonomy heat map for scenario #1.

6.2 Solar PV /Wind Turbine/Battery/ Electrolyzer /Hydrogen Tank (Scenario #2)

In scenario #2, in addition to solar, wind resources are also used to serve both hydrogen and electrical loads. In simulation scenario #2, the optimization results obtained are presented in **Table 5**. It is observed that solar PV has the highest capital cost, approximately 33.47% of the total system cost, followed by the electrolyzer (20.73%), battery unit (9.64%), and hydrogen tank (8.03%). The electrolyzer has the highest replacement costs, followed by the battery and other components. Solar PV has the highest operational and maintenance costs, followed by the electrolyzer, wind turbine, and battery. Following the project, the remaining power system components have a salvage value. **Figure 18** represents the cash flow of microgrid scenario #2 by component type in each year. The total NPC, the LCOE, and the LCOH all include the cost of solar PV, making it the most expensive source.

Table 5. Component cost summary and optimization result of scenario#2.

Component	Capital	Replace	O & M	Salvage	Total
Solar PV	$166,616	$0.00	$26,924	$0.00	$193,540
WT	$44,000	$14,028	$1,551	-$7,905	$51,673
Battery	$48,000	$20,365	$1,034	-$3,833	$65,566
Electrolyzer	$103,200	$22,062	$25,855	-$4,152	$146,965
HT	$40,000	$0.00	$0.00	$0.00	$40,000
Total	$401,816	$56,455	$55,365	-$15,891	$497,745

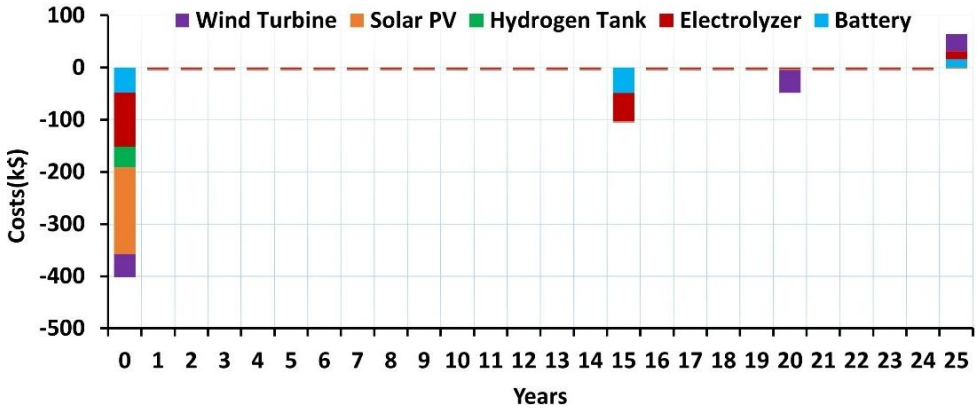

Figure 18. Cash flow of the microgrid scenario#2 by component type.

As seen in **Figure 19**, solar PV and wind turbines provide the entire year's sufficient supply of the load's energy needs. Solar energy makes a more significant contribution to the load than wind energy. **Table 3**

displays the detailed production and consumption of electrical energy. It can be observed that solar PV production is 90% of the total generation, and wind turbines produce 10% of the total production. Deferrable loads (6.59%), DC primary loads (23.6%), and electrolyzer all consume 69.9% of the total consumption. The excess energy is 16.5% (i.e., 120,737 kW/yr), with minimal capacity shortages and zero unmet electrical loads. The excess energy may be helpful for future loads. A total of 417 kW is the nominal capacity of the solar PV system. **Figure 20**, represents the annual energy production summary of Scenario #2 generation sources serves the hydrogen load. The yearly output of the 200 kW electrolyzer is 9,085 kg; a 200-kg capacity was chosen for the hydrogen tank. **Figure 21** represents the heat map of annual production, it represents the system produces 655,982 kWh annually, most of which is generated between 8:00 a.m. and 4:00 p.m. Power output from the wind turbine system, rated at 40.0 kW, is 74,906 kWh/yr. **Figure 22** represents the annual energy production of wind energy. The wind turbine output is higher in May, June, July, and August due to the location and environmental conditions. **Table 3** illustrates solar PV and wind turbine output data. The LCOE for solar PV is 0.0228 $ per kW, and the wind is 0.0534 $ per kWh.

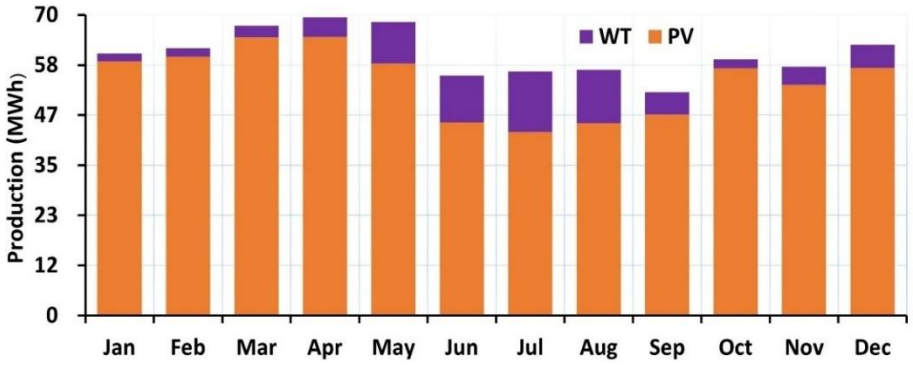

Figure 19. Annual energy production summary of integrated solar PV and wind for scenario #2.

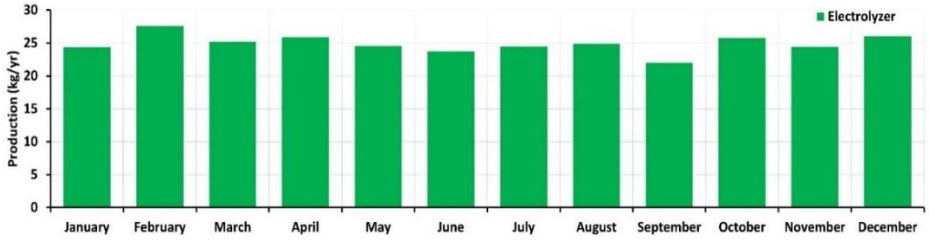

Figure 20. Annual energy production summary of electrolyzer scenario #2.

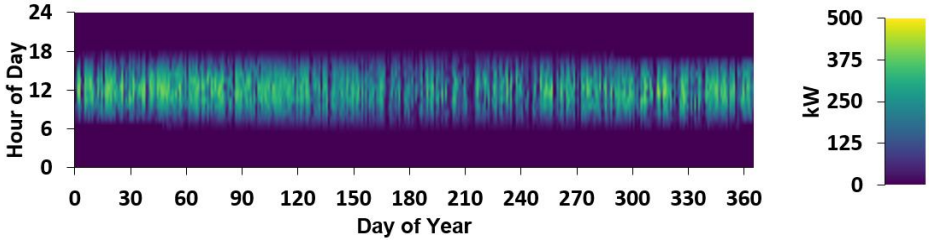

Figure 21. Annual solar production heat map for scenario #2.

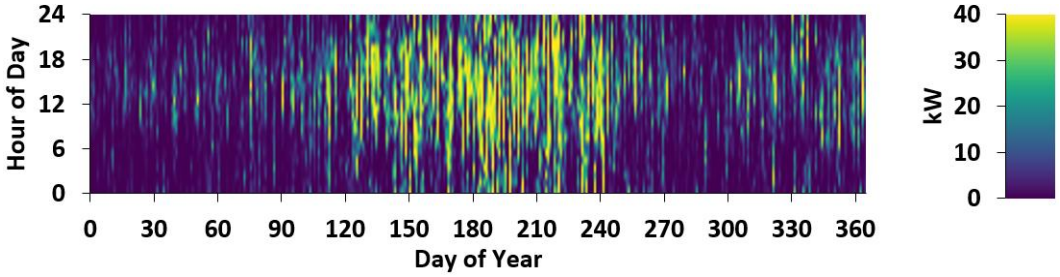

Figure 22. Annual energy production of wind turbines heat map for scenario #2.

The battery unit plays a significant role in a stand-alone system with intermittent power sources. The all-component specifications and statistics for scenario #2 are shown in **Table 5.** It provides data on the 400-kW lead-acid battery's various statistics, including the storage wear cost of 0.0422 $ per kWh. The battery unit's annual state of charge is depicted in **Figure 23**, and its estimated lifespan, based on the frequency with which it would be used, is roughly 15 years. The microgrid has a daily need of 25 kg and an hourly peak demand of 3.449 kg. **Figure 24**, illustrates the hydrogen tank's autonomy during the project's life cycle. It shows the overall cost of producing green hydrogen, including the LCOH of 4.24 $ per kilogram, the hydrogen load, the hydrogen tank, and the LCOE of 0.212 $ per kWh calculated.

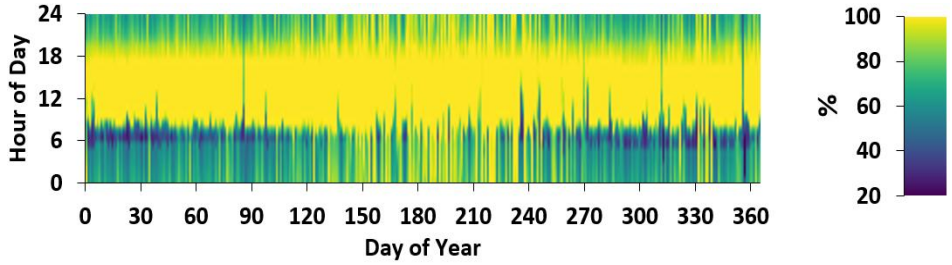

Figure 23. Annual State of charge of the battery unit heat map for scenario #2.

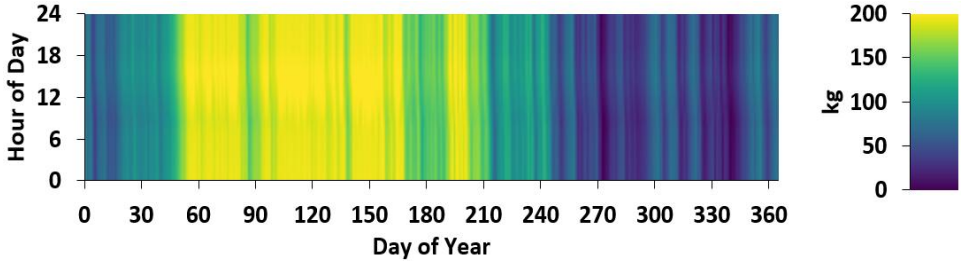

Figure 24. Annual hydrogen tank autonomy heat map for scenario #2.

6.3 Solar PV/Wind Turbine/Hydrokinetic Turbine/Battery/Electrolyzer/Hydrogen Tank (Scenario #3)

In scenario #3, hydroelectric resources are also used to serve hydrogen and electrical loads, as well as solar and wind. The optimization results obtained are presented in **Table 6.** It is observed that solar PV has the highest capital cost, approximately 27.82% of the total system cost, followed by the electrolyzer (22.23%),

hydrogen tank (8.61%), battery unit (7.75%), hydrokinetic turbine (7.53%), and wind turbine (4.73%). Electrolyzer costs dominate replacement costs. The electrolyzer has the highest operational and maintenance cost, followed by the solar PV and hydrokinetic turbine, while the wind turbine and battery have the same. The remaining power system components salvage value following the project. **Figure 25,** Represents the cash flow of microgrid scenario #3 by component type each year. The total NPC, the LCOE, and the LCOH all include the cost of solar PV, making it the most expensive source. As seen in **Figure 26**, solar PV, wind turbines, and hydrokinetic turbines provide the entire year's sufficient supply of the load's energy needs. Solar contributes more significantly to the load than hydrokinetics and wind. **Table 3** displays the detailed production and consumption of electrical energy. It observes that solar PV production accounts for 79.8% of total generation, hydrokinetic production for 14.30%, and wind turbine production for 5.88%. Deferrable loads (6.62%), DC primary loads (23.7%), and electrolyzer all consume 69.7% of the total consumption. The excess energy is 5.11% (i.e., 32,542 kW/yr.), with minimal capacity shortages and zero unmet electrical loads. The excess energy may be helpful for future loads.

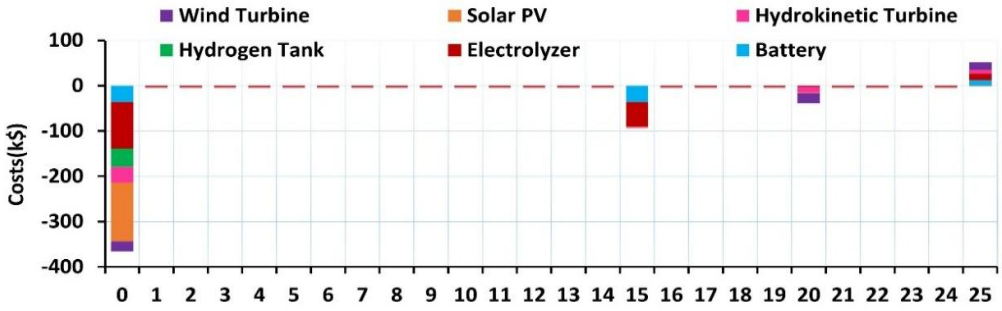

Figure 25. Cash flow of the microgrid scenario #3 by component type.

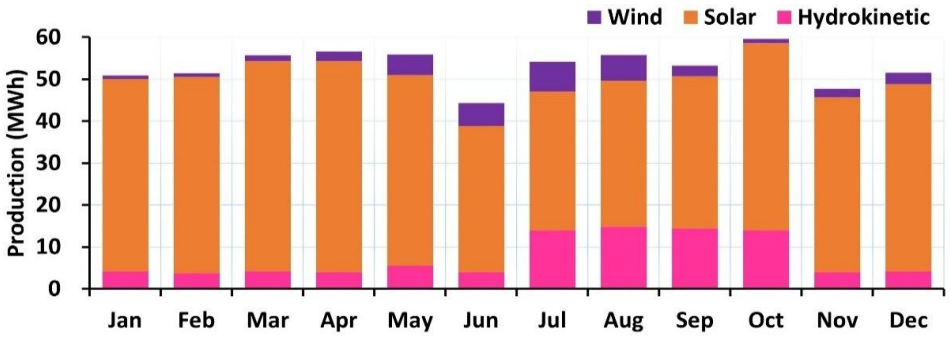

Figure 26. Annual energy production summary of integrated solar PV, wind, and hydrokinetic for scenario #3.

Table 6. Component cost summary and optimization result of scenario #3.

Component	Capital	Replace	O & M	Salvage	Total
Solar PV	$129,182	$0.00	$20,875	$0.00	$150,057
WT	$22,000	$7,014	$775.65	-$3,953	$25,837
HKT	$35,000	$3,826	$15,513	-$2,156	$52,183
Battery	$36,000	$15,274	$775.65	-$2,875	$49,175
Electrolyzer	$103,200	$22,062	$25,855	-$4,152	$146,965
HT	$40,000	$0.00	$0.00	$0.00	$40,000
Total	**$365,382**	**$48,176**	**$63,794**	**-$13,136**	**$464,216**

A total of 323 kW is the nominal capacity of the solar PV system. The annual energy production summary of Scenario #3 generation sources serves the hydrogen load shown in **Figure 27.** The yearly output of the 200 kW electrolyzer is 9,085 kg; a 200-kg capacity was chosen for the hydrogen tank. **Figure 28,** represents the heat map of the annual production system; it produces 508,600 kWh annually, with most of that being generated between 8:00 a.m. and 4:00 p.m. Power output from the wind turbine system, rated at 20 kW, is 37,453 kWh/yr. **Figure 29,** represents the annual energy production of wind energy. Due to environmental conditions, the wind turbine output is higher in May, June, July, and August. The hydrokinetic turbine has a total rated capacity of 20.0 kW. The total annual production is 90,926 kWh/year, with most of it generated in July, August, September, and October due to the rainy season, and the remaining months generate the minimum amount of energy. **Figure 30,** represents the annual hydrokinetic energy production. The LCOE for solar PV is 0.0228 $ per kW, the wind is 0.0534 $ per kW, and the hydrokinetic is 0.0444 $ per kW. The 200-kWh lead-acid battery's various statistics, including the storage wear cost of 0.0422 $ per kWh, are shown in **Table 3**. **Figure 31,** presents the battery unit's annual state of charge, and its estimated lifespan, based on the frequency with which it would be used, is roughly 15 years. The microgrid has a daily need of 25 kg and an hourly peak demand of 3.449 kg. **Figure 32**, illustrates the hydrogen tank's autonomy during the project's life cycle. It shows the overall cost of producing green hydrogen, including the LCOH of 3.98 $ per kilogram, the hydrogen load, and the hydrogen tank, and the LCOE of 0.197 $ per kWh is calculated.

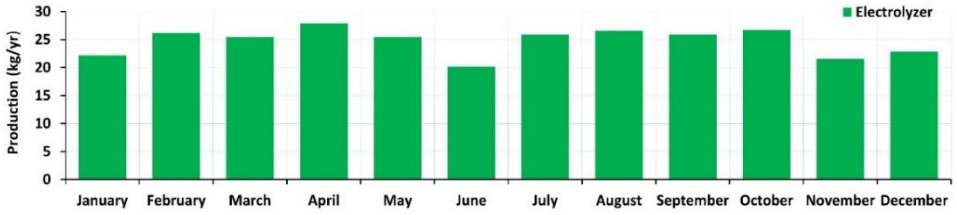

Figure 27. Annual energy production summary of electrolyzer for scenario #3.

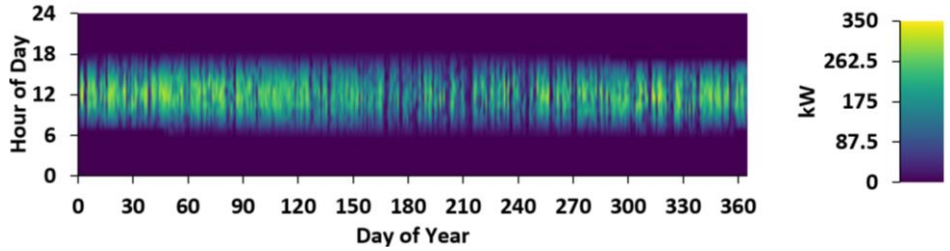

Figure 28. Annual solar production heat map for scenario #3.

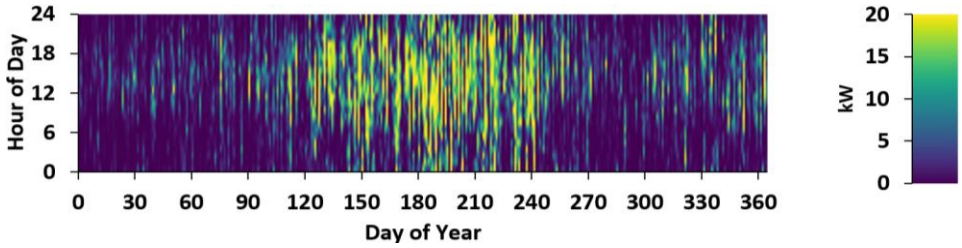

Figure 29. Annual energy production from wind turbines heat map for scenario #3.

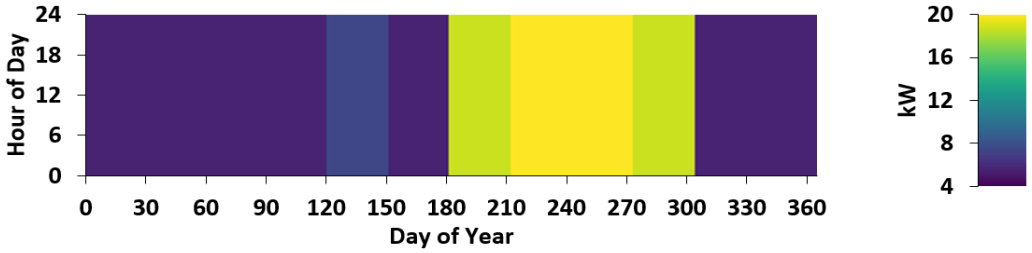

Figure 30. Annual energy production from hydrokinetic energy turbines heat map for scenario #3.

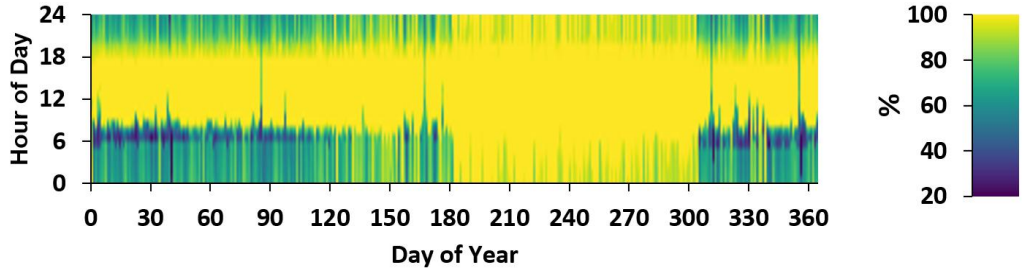

Figure 31. Annual state of charge of the battery unit heat map for scenario #3.

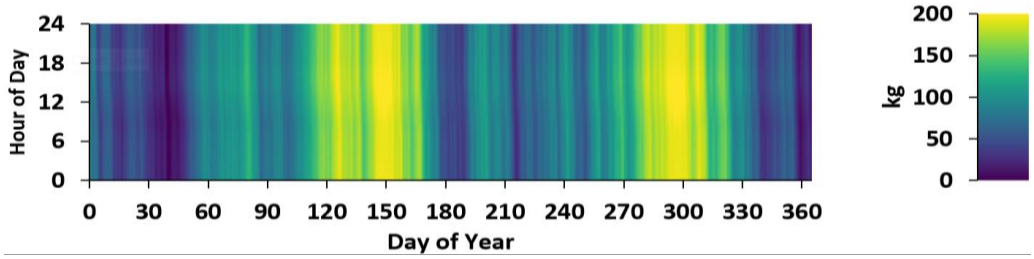

Figure 32. Annual hydrogen tank autonomy heat map for scenario #3.

6.4 Comparative Analysis

A comparative analysis is performed concerning the three scenarios based on the optimal economic and technical parameters shown in **Table 3**. **Figure 33** presents a detailed cost summary of the three microgrid scenarios, and **Figures 34, 35,** and **36**. Optimal parameters enhance microgrids, helping to improve their performance in terms of efficient energy generation, load matching, and economic viability. Economic parameters assessing the financial feasibility and economic benefits of implementing a microgrid include cost-benefit analysis, energy cost savings, tariff and rate analysis, financing options, and project viability. Technical parameters in a microgrid system determine how the microgrid functions, its reliability, and its ability to meet energy demands efficiently in terms of renewable energy integration, load shedding and prioritization, islanding and resynchronization, and energy storage management.

The electrolyzer and hydrogen tank have the same ratings in the three scenarios. The following points are from the comparative analysis between the three scenarios. In scenario #1, only using solar, the power rating of the solar PV is 31.6%, and the battery capacity is 20%, which is lower than in scenario #2. NPC, LCOE, and LCOH also produce a lot of excess energy. In terms of optimal technical and economic

resources, there is a significant gap compared to the other two cases. The final ranking for this scenario is three.

Scenario #2 integrates solar and wind power, resulting in 22.4% higher solar PV ratings and 50% higher wind power than Scenario #3. Battery capacity is 20% lower than in Scenario #1 and 20% higher than in Scenario #3. This results in more cost-effective and environmentally friendly energy generation than Scenario #1 and less than Scenario #3, as measured by the NPC, LCOE, and LCOH. The final ranking for this scenario is two.

Scenario #3 integrates solar, wind, and hydropower resources. Even if the battery capacity is 20%, wind power is 50% lower than in Scenario #2. However, incorporating the HKT turbine, the total power rating from all three sources continues to archive the load demand with minimum excess energy and capacity shortage. NPC, LCOE, and LCOH costs are lower than those of the remaining two scenarios. The final ranking for this scenario is one.

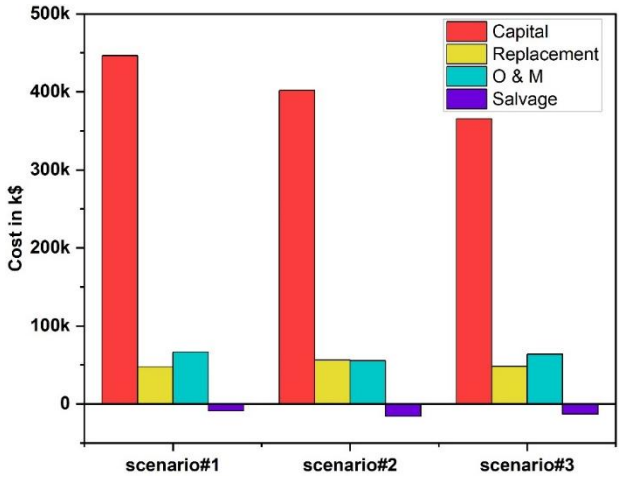

Figure 33. Cost summary comparisons of three microgrid scenarios.

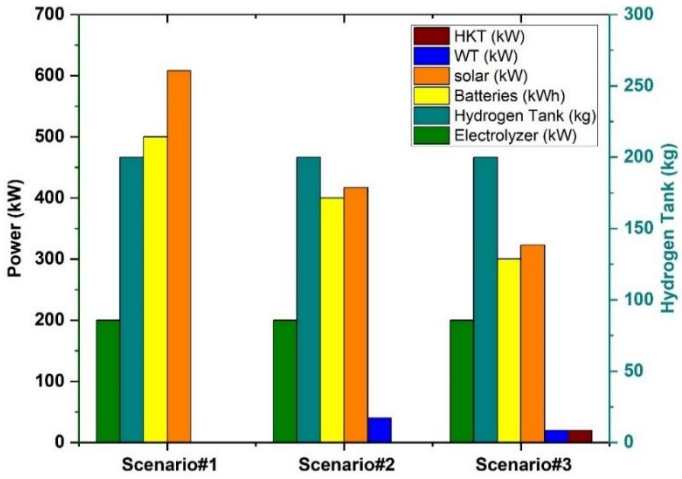

Figure 34. Optimal parameters comparisons of three microgrid scenarios.

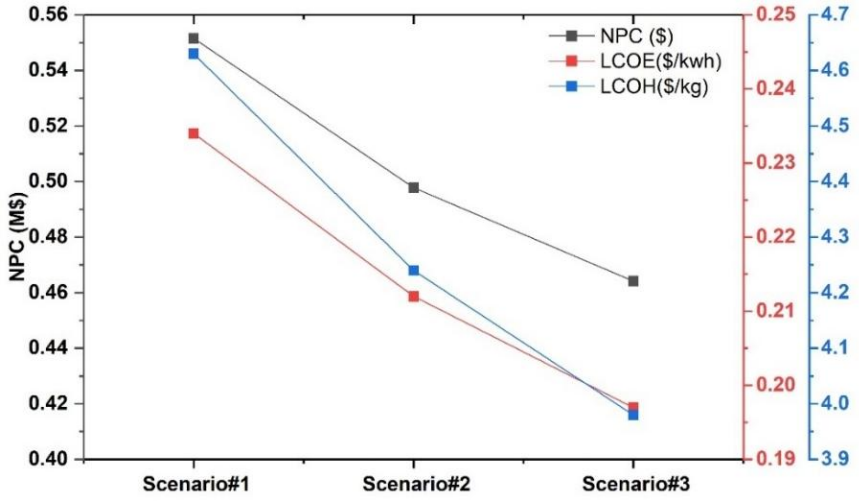

Figure 35. Economic parameters comparisons of three microgrid scenarios.

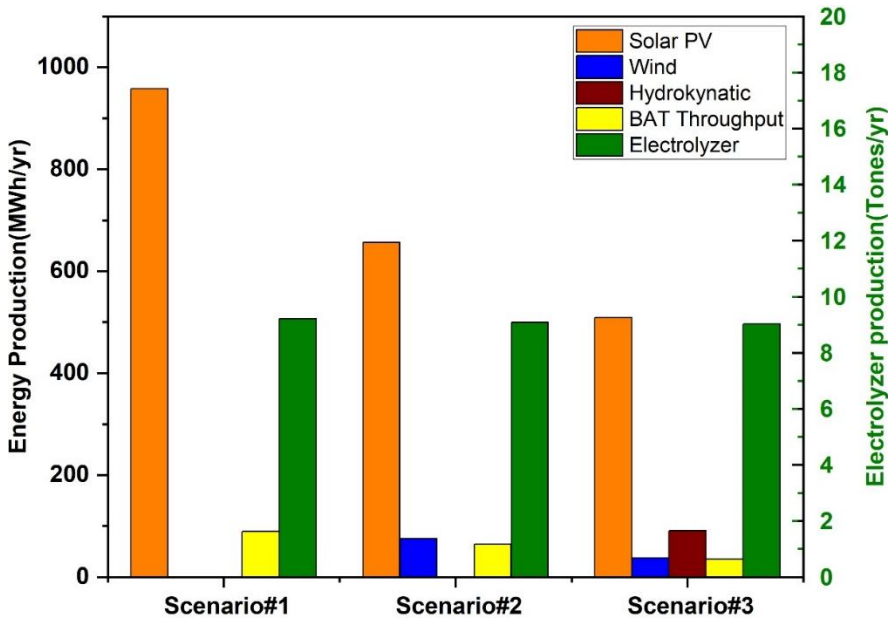

Figure 36. Technical parameters comparisons of three microgrid scenarios.

The proposed model for combined energy generation and supply of electricity and hydrogen is stable and affordable compared to previous studies. The model demonstrates novelty and outperforms existing literature regarding minimal economy (NPC and LCOE). **Table 7** provides a matrix of energy system compatibility and hydrogen production methods, highlighting the most promising technologies and energy sources from an Indian perspective. This comparison emphasizes the role of hydrokinetic turbines, along with solar wind resources, in reducing LCOE and LCOH and offering reliability over other integrated microgrids.

Table 7. DC microgrid component's specification and statistics for three scenarios with the electricity and hydrogen utility.

References	Location	Energy resources	Total load (kWh/Day)	Peak load (kWh/Day)	NPC (million $)	LCOE ($/kwh)	LCOH ($/kg)
Das et al. (2024)	India	DG/Solar/wind	515	61.44	0.8	0.252	2.59
Yadav et al. (2024)	India	Solar/wind	520.39	50.31	0.83	0.232	36.6
Alluraiah and Vijayapriya (2023)	India	DG/Solar/wind	704.89	77.67	11	0.78	20.7
Praveenkumar et al. (2022)	India	Solar	1500	186	2.4	0.41	3.22
Present	**India**	**Solar/Wind/HKT**	**498.74**	**66.32**	**0.43**	**0.197**	**3.98**

6.5 Reliability Analysis

The reliability analysis will help the microgrid in energy security, system resilience, optimizing component sizing, reducing operational costs, and reducing load demand inconsistency. Additionally, DC microgrid performance indicators and optimal design are investigated using reliability analysis. The key factors, such as capacity shortage factor (CSF) and energy storage systems, influence the reliability of the hybrid microgrid. The component sizes are optimized while accounting for CSF values ranging from 5% to 10% annually. Consequently, **Figure 37** and **Table 8** represent the outcomes of the reliability study.

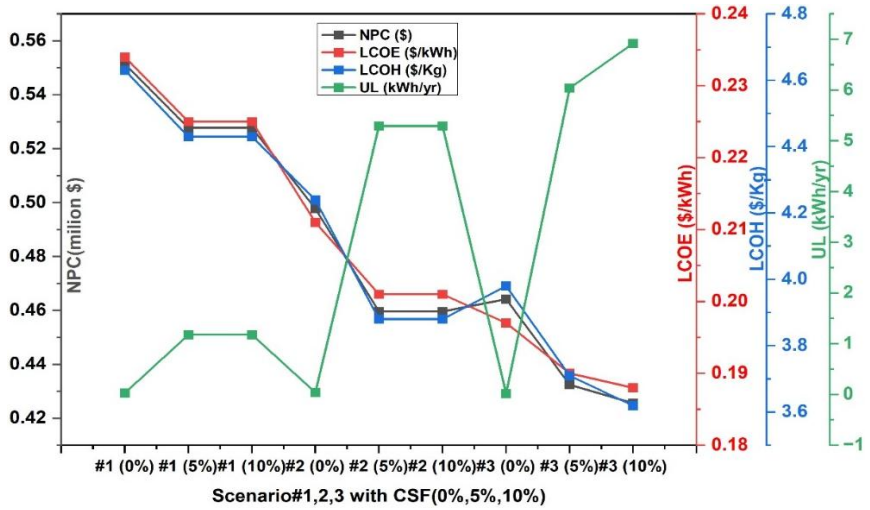

Figure 37. Effect of CSF% variation on the microgrid's economic and energy performance indicators.

In scenario #1, CSF is increasing to 5%, and the corresponding NPC, LCOE, and LCOH are decreasing to 0.527 million dollars, 0.225 $/kWh, and 4.43 $/kg, respectively, with an increase in unmet loads of 1178 kWh per year. In this case, the number of PV arrays decreased to 604 kW, and three 100 kWh batteries of the same 200 kW EL and 200kg HT were used. Furthermore, the CSF is increasing to 10%, corresponding to the same 5% reduction. In scenario #2, CSF is increasing to 5%, and the corresponding NPC, LCOE, and LCOH are decreasing to 0.45 million dollars, 0.201 dollars per kWh, and 3.88 dollars per kg, with an increase in unmet loads of 5290 kWh per year. In this case, the number of PV arrays decreased to 416 kW, increased to 5 WT, and decreased to two 100 kWh batteries with the same 200 kW EL and 100 kg HT. Moreover, the CSF is increasing to 10%, corresponding to the same 5% reduction. Similarly, in scenario #3, CSF is increasing to 5%, and the corresponding NPC, LCOE, and LCOH are decreasing to 0.43 million dollars, 0.190 dollars per kWh, and 3.71 dollars per kg, with an increase in unmet loads of 6040 kWh per year. In this case, the number of PV arrays decreased to 298 kW, increased to 3 WT, and decreased to one

100 kWh battery with the same 200 kW EL and 200 kg HT. Again, the CSF is increasing to 10%, and the corresponding NPC, LCOE, and LCOH are decreasing to 0.42 million dollars, 0.188 dollars per kWh, and 3.62 dollars per kg, with an increase in unmet loads of 6919 kWh per year. In this case, the number of PV arrays decreased to 311 kW, the WT decreased to 210 kW, the same as the 20 kW HKT, and the battery decreased to one 100 kWh of the same 200 kW EL and 200kg HT.

Table 8. Optimal technical and economical design capabilities for CSF variation.

Scenario	Optimal design capacities							Economical design capacities			Technical design capacities				
	CSF (%)	PV (kW)	WT (#)	BAT (#)	HKT (#)	EL (kW)	HT (kg)	NPC (million$)	LCOE ($/kWh)	LCOH ($/Kg)	UL (kWh/yr)	PV/Energy production (MWh/yr)	WT/ Production (kWh/yr)	Battery/ Annual throughput (kWh/yr)	HKT/ Mean output (kW)
#1	5	604	---	3	---	200	200	0.527	0.225	4.43	1178	951	0	83	0
#2	5	416	5	2	---	200	100	0.459	0.201	3.88	5290	654	94	46	0
#3	5	298	3	1	1	200	200	0.432	0.19	3.71	6040	469	57	19	11
#1	10	604	---	3	---	200	200	0.527	0.225	4.43	1178	951	0	83	0
#2	10	416	5	2	---	200	100	0.459	0.201	3.88	5290	654	94	46	0
#3	10	311	2	1	1	200	200	0.425	0.188	3.62	6919	489	38	20	11

The feasibility study has encountered significant site-specific challenges, including resource availability (such as solar, wind, and HKT sources), geographic limitations, and infrastructure accessibility. Technology scalability, the proposed system is designed for small-scale remote community applications; scaling up such systems for larger communities or industrial applications may require additional considerations related to infrastructure and system control. Economic uncertainties, the microgrid system is subject to fluctuations in the cost of renewable technologies, energy storage systems, and maintenance. For future research directions, a small-scale prototype experimental validation model in a real-world setting. Advanced control strategies such as artificial intelligence-based predictive energy management help improve the system's efficiency and reliability. A small-scale prototype for real-world validation and integration of advanced energy management algorithms to improve the system efficiency for further research.

7. Conclusions

This article investigated the feasibility, planning, optimal, technical, and economic analysis of solar, wind, and hydrokinetic energy with battery storage-based standalone DC microgrids to produce green hydrogen and electricity for remote area applications. Based on simulation results, Solar PV, wind, and hydrokinetic energy-based microgrids (Scenario #3) were identified as the best optimal configuration system, offering the lowest NPC, LCOE, and LCOH than standalone solar PV or solar-wind hybrid configurations. Sensitivity analysis was also conducted by considering 0%, 5%, and 10% capacity shortage fractions to enhance the reliability. A comprehensive opto-techno-economic analysis was considered for energy demand, resource availability, and minimizing the system components by using HOMER Pro. The study's main contribution is understanding energy planning for remote areas by considering the available renewable energy sources to produce green hydrogen and electricity for their load requirements. The microgrid system is subject to fluctuations in the cost of renewable technologies, energy storage systems, and maintenance. Also, skilled employers are required to handle the hydrogen. For future research directions, a small-scale prototype experimental validation model in a real-world setting. Advanced control strategies such as artificial intelligence-based predictive energy management help improve the system's efficiency and reliability.

Conflict of Interest
The authors confirm that there is no conflict of interest to declare for this publication.

Acknowledgments
This research did not receive any specific grant from funding agencies in the public, commercial, or not-for-profit sectors. The authors would like to thank the editor and anonymous reviewers for their comments that helped improve the quality of this work.

AI Disclosure
The author(s) declare that no assistance is taken from generative AI to write this article.

References

Al-Ghussain, L., Ahmad, A.D., Abubaker, A.M., & Hassan, M.A. (2022). Exploring the feasibility of green hydrogen production using excess energy from a country-scale 100% solar-wind renewable energy system. *International Journal of Hydrogen Energy*, *47*(51), 21613-21633. https://doi.org/10.1016/j.ijhydene.2022.04.289.

Alluraiah, N.C., & Vijayapriya, P. (2023). Optimization, design, and feasibility analysis of a grid-integrated hybrid AC/DC microgrid system for rural electrification. *IEEE Access*, *11*, 67013-67029.

Al-Orabi, A.M., Osman, M.G., & Sedhom, B.E. (2023a). Analysis of the economic and technological viability of producing green hydrogen with renewable energy sources in a variety of climates to reduce CO_2 emissions: a case study in Egypt. *Applied Energy*, *338*, 120958. https://doi.org/10.1016/j.apenergy.2023.120958.

Al-Orabi, A.M., Osman, M.G., & Sedhom, B.E. (2023b). Evaluation of green hydrogen production using solar, wind, and hybrid technologies under various technical and financial scenarios for multi-sites in Egypt. *International Journal of Hydrogen Energy*, *48*(98), 38535-38556. https://doi.org/10.1016/j.ijhydene.2023.06.218.

Al-Shetwi, A.Q., Atawi, I.E., Abuelrub, A., & Hannan, M.A. (2023). Techno-economic assessment and optimal design of hybrid power generation-based renewable energy systems. *Technology in Society*, *75*, 102352. https://doi.org/10.1016/j.techsoc.2023.102352.

Amoussou, I., Tanyi, E., Fatma, L., Agajie, T.F., Boulkaibet, I., Khezami, N., Ali, A. & Khan, B. (2023). The optimal design of a hybrid solar PV/wind/hydrogen/lithium battery for the replacement of a heavy fuel oil thermal power plant. *Sustainability*, *15*(15), 11510. https://doi.org/10.3390/su151511510.

Bakeer, A., Elmorshedy, M.F., Salama, H.S., Elkadeem, M.R., Almakhles, D.J., & Kotb, K.M. (2023). Optimal design and performance analysis of coastal microgrid using different optimization algorithms. *Electrical Engineering*, *105*(6), 4499-4523. https://doi.org/10.1007/s00202-023-01954-9.

Brown, D., Dahlan, N., & Richardson-Barlow, C. (2024). Evaluating microgrid business models for rural electrification: a novel framework and three cases in Southeast Asia. *Energy for Sustainable Development*, *80*, 101443. https://doi.org/10.1016/j.esd.2024.101443.

Cano, A., Arévalo, P., & Jurado, F. (2020). Energy analysis and techno-economic assessment of a hybrid PV/HKT/BAT system using biomass gasifier: Cuenca-Ecuador case study. *Energy*, *202*, 117727. https://doi.org/10.1016/j.energy.2020.117727.

Dandupati, G., Chodavarapu, S., Chalumuri, R.N., & Ahirwar, A. (2024). Runoff modeling with various unit-hydrograph approaches for Sarada river basin, India. *Arabian Journal of Geosciences*, *17*(5), 150.

Das, S., De, S., Dutta, R., & De, S. (2024). Multi-criteria decision-making for techno-economic and environmentally sustainable decentralized hybrid power and green hydrogen cogeneration system. *Renewable and Sustainable Energy Reviews*, *191*, 114135. https://doi.org/10.1016/j.rser.2023.114135.

Elavarasan, R.M., Nadarajah, M., Pugazhendhi, R., Sinha, A., Gangatharan, S., Chiaramonti, D., & Houran, M.A. (2023). The untold subtlety of energy consumption and its influence on policy drive towards sustainable development goal 7. *Applied Energy*, *334*, 120698. https://doi.org/10.1016/j.apenergy.2023.120698.

Elmorshedy, M.F., Elkadeem, M.R., Kotb, K.M., Taha, I.B., El-Nemr, M.K., Kandeal, A.W., Sharshir, S.W., Almakhles, D.J., & Imam, S.M. (2022). Feasibility study and performance analysis of microgrid with 100% hybrid renewables for a real agricultural irrigation application. *Sustainable Energy Technologies and Assessments*, *53*(D), 102746. https://doi.org/10.1016/j.seta.2022.102746.

Hasan, T., Emami, K., Shah, R., Hassan, N.M.S., Belokoskov, V., & Ly, M. (2023). Techno-economic assessment of a hydrogen-based islanded microgrid in north-east. *Energy Reports*, *9*, 3380-3396. https://doi.org/10.1016/j.egyr.2023.02.019.

Homer (2024). *Homer pro-standalone microgrids*. Retrieved from https://homerenergy.com/products/pro/index.html.

Hoseinzadeh, S., Garcia, D.A., & Huang, L. (2023). Grid-connected renewable energy systems flexibility in Norway islands' Decarbonization. *Renewable and Sustainable Energy Reviews*, *185*, 113658. https://doi.org/10.1016/j.rser.2023.113658.

Irshad, A.S., Samadi, W.K., Fazli, A.M., Noori, A.G., Amin, A.S., Zakir, M.N., Bakhtyal, I.A., Karimi, B.A., Ludin, G.A., & Senjyu, T. (2023). Resilience and reliable integration of PV-wind and hydropower based 100% hybrid renewable energy system without any energy storage system for inaccessible area electrification. *Energy*, *282*, 128823. https://doi.org/10.1016/j.energy.2023.128823.

Jahangiri, M., Soulouknga, M.H., Bardei, F.K., Shamsabadi, A.A., Akinlabi, E.T., Sichilalu, S.M., & Mostafaeipour, A. (2019). Techno-econo-environmental optimal operation of grid-wind-solar electricity generation with hydrogen storage system for domestic scale, case study in Chad. *International Journal of Hydrogen Energy*, *44*(54), 28613-28628. https://doi.org/10.1016/j.ijhydene.2019.09.130.

Jahannoush, M., & Nowdeh, S.A. (2020). Optimal designing and management of a stand-alone hybrid energy system using meta-heuristic improved sine-cosine algorithm for recreational center, case study for Iran country. *Applied Soft Computing*, *96*, 106611. https://doi.org/10.1016/j.asoc.2020.106611.

Kapen, P.T., Nouadje, B.A.M., Chegnimonhan, V., Tchuen, G., & Tchinda, R. (2022). Techno-economic feasibility of a PV/battery/fuel cell/electrolyzer/biogas hybrid system for energy and hydrogen production in the far north region of cameroon by using HOMER pro. *Energy Strategy Reviews*, *44*, 100988.

Manoo, M.U., Shaikh, F., Kumar, L., & Arıcı, M. (2024). Comparative techno-economic analysis of various stand-alone and grid connected (solar/wind/fuel cell) renewable energy systems. *International Journal of Hydrogen Energy*, *52*, 397-414. https://doi.org/10.1016/j.ijhydene.2023.05.258.

Modu, B., Abdullah, M.P., Bukar, A.L., Hamza, M.F., & Adewolu, M.S. (2023a). Energy management and capacity planning of photovoltaic-wind-biomass energy system considering hydrogen-battery storage. *Journal of Energy Storage, 73*, 109294. https://doi.org/10.1016/j.est.2023.109294.

Modu, B., Abdullah, M.P., Sanusi, M.A., & Hamza, M.F. (2023b). DC-based microgrid: topologies, control schemes, and implementations. *Alexandria Engineering Journal*, *70*, 61-92. https://doi.org/10.1016/j.aej.2023.02.021.

Mulenga, E., Kabanshi, A., Mupeta, H., Ndiaye, M., Nyirenda, E., & Mulenga, K. (2023). Techno-economic analysis of off-grid PV-diesel power generation system for rural electrification: a case study of Chilubi district in Zambia. *Renewable Energy*, *203*, 601-611. https://doi.org/10.1016/j.renene.2022.12.112.

Ngouleu, C.A.W., Koholé, Y.W., Fohagui, F.C.V., & Tchuen, G. (2023). Techno-economic analysis and optimal sizing of a battery-based and hydrogen-based standalone photovoltaic/wind hybrid system for rural electrification in Cameroon based on meta-heuristic techniques. *Energy Conversion and Management*, *280*, 116794.

Noruzi, R., Vahidzadeh, M., & Riasi, A. (2015). Design, analysis and predicting hydrokinetic performance of a horizontal marine current axial turbine by consideration of turbine installation depth. *Ocean Engineering*, *108*, 789-798. https://doi.org/10.1016/j.oceaneng.2015.08.056.

Phurailatpam, C., Rajpurohit, B.S., & Wang, L. (2018). Planning and optimization of autonomous DC microgrids for rural and urban applications in India. *Renewable and Sustainable Energy Reviews*, *82*, 194-204.

Praveenkumar, S., Agyekum, E.B., Ampah, J.D., Afrane, S., Velkin, V.I., Mehmood, U., & Awosusi, A.A. (2022). Techno-economic optimization of PV system for hydrogen production and electric vehicle charging stations under five different climatic conditions in India. *International Journal of Hydrogen Energy*, *47*(90), 38087-38105.

Puppala, S., Singh, P.P., & Potnuru, D. (2024). Standalone solar photovoltaic systems for remote area applications: a bibliometric and feasibility analysis. In: Panda, G., Basu, M., Siano, P., Affijulla, S. (eds) *Proceedings of Third International Symposium on Sustainable Energy and Technological Advancements*. Springer, Singapore.

Puppala, S., Singh, P.P., & Potnuru, D. (2025). Investigating the feasibility of a renewable energy-based standalone microgrid for remote area applications: An opto-techno-economic and environmental perspective. *Environmental Engineering Research*, *30*(3), 240340. https://doi.org/10.4491/eer.2024.340.

Rad, M.A.V., Ghasempour, R., Rahdan, P., Mousavi, S., & Arastounia, M. (2020). Techno-economic analysis of a hybrid power system based on the cost-effective hydrogen production method for rural electrification, a case study in Iran. *Energy*, *190*, 116421. https://doi.org/10.1016/j.energy.2019.116421.

Salhi, M.S., Okonkwo, P.C., Belgacem, I.B., Farhani, S., Zghaibeh, M., & Bacha, F. (2023). Techno-economic optimization of wind energy based hydrogen refueling station case study Salalah city Oman. *International Journal of Hydrogen Energy*, *48*(26), 9529-9539. https://doi.org/10.1016/j.ijhydene.2022.12.148.

Turkdogan, S. (2021). Design and optimization of a solely renewable based hybrid energy system for residential electrical load and fuel cell electric vehicle. *Engineering Science and Technology, an International Journal*, *24*(2), 397-404. https://doi.org/10.1016/j.jestch.2020.08.017.

Vakili, S., & Ölçer, A.I. (2023). Techno-economic-environmental feasibility of photovoltaic, wind and hybrid electrification systems for stand-alone and grid-connected port electrification in the Philippines. *Sustainable Cities and Society*, *96*, 104618. https://doi.org/10.1016/j.scs.2023.104618.

Veilleux, G., Potisat, T., Pezim, D., Ribback, C., Ling, J., Krysztofiński, A., Ahmed, A., Papenheim, J., Pineda, A.M., Sembian, S., & Chucherd, S. (2020). Techno-economic analysis of microgrid projects for rural electrification: A systematic approach to the redesign of Koh Jik off-grid case study. *Energy for Sustainable Development*, *54*, 1-13. https://doi.org/10.1016/j.esd.2019.09.007.

Vermaak, H.J., Kusakana, K., & Koko, S.P. (2014). Status of micro-hydrokinetic river technology in rural applications: A review of literature. *Renewable and Sustainable Energy Reviews*, *29*, 625-633.

Xia, T., Rezaei, M., Dampage, U., Alharbi, S.A., Nasif, O., Borowski, P.F., & Mohamed, M.A. (2021). Techno-economic assessment of a grid-independent hybrid power plant for co-supplying a remote micro-community with electricity and hydrogen. *Processes*, *9*(8), 1375. https://doi.org/10.3390/pr9081375.

Yadav, S., Kumar, P., & Kumar, A. (2024). Techno-economic assessment of hybrid renewable energy system with multi energy storage system using HOMER. *Energy*, *297*, 131231. https://doi.org/10.1016/j.energy.2024.131231.

Zeyad, M., Ahmed, S.M., Hasan, S., & Mahmud, D.M. (2023). Community microgrid: an approach towards positive energy community in an urban area of Dhaka, Bangladesh. *Clean Energy*, *7*(4), 926-939.